

**Experimental Validation of Composite Solid  
Propellant Burning Rate Prediction Model  
(He-Qu-1D) using Ultrasonic Burning Rate (UBR)**

Shaik Mujeeb

ME17MTECH11002

A thesis Submitted to  
Indian Institute of Technology Hyderabad  
In Partial Fulfillment of the Requirements for  
The Degree of Master of Technology



भारतीय प्रौद्योगिकी संस्थान हैदराबाद  
Indian Institute of Technology Hyderabad

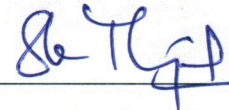
Department of Mechanical and Aerospace Engineering

July 2019



## Declaration

I declare that this written submission represents my ideas in my own words, and where ideas or words of others have been included, I have adequately cited and referenced the original sources. I also declare that I have adhered to all principles of academic honesty and integrity and have not misrepresented or fabricated or falsified any idea/data/fact/source in my submission. I understand that any violation of the above will be a cause for disciplinary action by the Institute and can also evoke penal action from the sources that have thus not been properly cited, or from whom proper permission has not been taken when needed.



(Signature)

SHAIK MUJEEB

(Shaik Mujeeb)

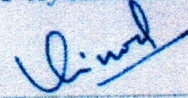
ME17MTECH11002

(Roll No.)

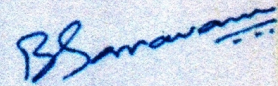


## Approval Sheet

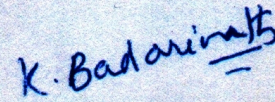
This thesis entitled Experimental Validation of Composite Solid Propellant Burning Rate Prediction Model (He-Qul-D) using Ultrasonic Burning Rate (UBR) by Shaik Mujeeb is approved for the degree of Master of Technology from IIT Hyderabad.



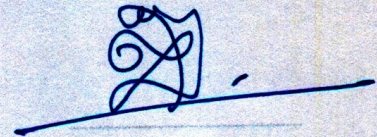
(Dr. Vinod Janardhanan) Examiner & Chairman  
Dept. of Chemical Engineering  
IITH



(Dr. Saravanan Balusamy) Examiner  
Dept. Mechanical and Aerospace Engineering  
IITH



(Dr. Badarinath Karri) Advisor  
Dept. of Mechanical and Aerospace Engineering  
IITH



(Dr. Jeenu R ) Co-Advisor  
Group Head, Solid Motors Group  
VSSC/ISRO



## Acknowledgements

I would first like to thank my thesis advisors Dr. Badarinath Karri, Assistant Professor, Department of Mechanical Aerospace Engineering at Indian Institute of Technology, Hyderabad, and Dr. Jeenu R, Group Head, Solid Motors Group, VSSC / ISRO. They were always available for discussion whenever I ran into a trouble spot or had a question about my research or writing. Their valuable suggestions and guidance has lead to pursue this project more fruitfully.

I am grateful to Dr. Varunkumar S, Assistant Professor, IIT, Madras for lending his MATLAB code of the model and for giving valuable suggestions and review of this project very closely without which this project would not have been completed

I am very grateful to Smt. Elizabeth John, Group Director, Propellant and Special Chemicals Group and Shri Suraj S, Head, Propellant Engineering Division for their motivation and untiring support to complete this project and also thank Dr. Reshmi S and Shri Bhatt Tushar Shriram and all my colleges of Propellant Engineering Division, VSSC for their support and guidance to complete all the experiments without any hindrance. I would like to specially thank Dr. Lakshmi VM, DGM, PRMF for her guidance and support to complete the particle size analysis in RPP. I also would like to thank my colleagues of Analytical and Spectroscopy Division, VSSC for their help in completing the particle size analysis at ASD. I am also grateful to Shri Kiran Pinumalla, GNDD, VSSC for his valuable suggestions throughout the project.

I would also like to thank Deputy Director, VSSC(PCM) for allowing me to pursue masters program in IIT, Hyderabad and Director VSSC for granting permission and leave to complete the masters program in IIT, Hyderabad successfully.

I am in debted to my post graduate test committee members, Dr. Saravanan Balusamy and Dr. Vinod janardhana for their valuable comments and suggestions on the project work.

I would also like to thank my friends in IIT, Hyderabad for making my two years as a masters student truly memorable. I would also acknowledge the love and support rendered by my family and friends throughout this endeavour.

## Abstract

A valid predictive tool of ballistic behaviour of composite solid propellant gives more advantage for a designer of solid propellant to freeze a composition for a particular application. Composite solid propellant in ISRO is composed of major fraction of ammonium perchlorate (AP) as oxidizer and hydroxyl terminated polybutadine (HTPB) as the fuel-cum-binder. In this work, attempt has been made to validate one of the latest burning rate prediction models: heterogeneous quasi one dimensional model (He-Qu-1D) developed at IIT, Madras utilizing ISRO compositions of solid propellant. Thus this model can be used for the new compositions development in ISRO, and invariably reducing the trails for the optimization of the composition. Composite solid propellant combustion is determined by the diffusion and premixing of decomposition products of AP and HTPB binder where the binder is surrounded around the AP particle. Hence, the particle size distribution of AP is very crucial information for solid propellant combustion modelling. In view of this, different techniques of particle size distribution viz., sieve analysis, laser scatter dry method, laser scatter wet method, image analysis has been explored and studied in detail to determine the best method for repeated measurement. Based on this standardized method of measurement, particle size distribution information of AP, is measured and is fed to the above said He-Qu-1D model and predictions were made for six compositions of propellants. The results thus obtained were compared with the ultrasonic burning rates (UBR) results measured experimentally. Details of these results are discussed in this report. It is observed that there is a good agreement between the prediction and experimental results of major compositions.

# Contents

Declaration . . . . .	ii
Approval Sheet . . . . .	iv
Acknowledgements . . . . .	v
Abstract . . . . .	vi
<b>List of Figures</b>	<b>5</b>
<b>List of Tables</b>	<b>6</b>
<b>Nomenclature</b>	<b>7</b>
<b>1 Introduction</b>	<b>7</b>
1.1 Literature review . . . . .	8
1.1.1 Particle size distribution of Ammonium Perchlorate . . . . .	8
1.1.2 Modelling of combustion of composite solid propellant and its prediction of ballistic behaviour . . . . .	10
1.2 Outline of the thesis . . . . .	11
<b>2 Ammonium Perchlorate and its particle size characterization</b>	<b>13</b>
2.1 Ammonium Perchlorate . . . . .	13
2.2 Particle size distribution . . . . .	14
2.2.1 Sieve analysis . . . . .	15
2.2.2 Microscopic method and image analysis . . . . .	15
2.2.3 Laser scatter method . . . . .	15
2.3 Laser diffraction particle size analyser . . . . .	16
2.3.1 Dry method . . . . .	17
2.3.2 Wet method . . . . .	17
2.4 Particle size analysis using different techniques and results . . . . .	18
2.4.1 Sieve analysis . . . . .	19
2.4.2 Microscopic method . . . . .	19



---

2.4.3	Laser scatter - Wet analysis . . . . .	21
2.5	Comparison of Particle size distribution analysed by different techniques . . . . .	31
2.5.1	Sieve analysis and laser diffraction techniques . . . . .	31
2.5.2	Microscopic (image analysis) and Laser scatter techniques . . . . .	32
2.6	Representation of particle size distribution . . . . .	34
<b>3</b>	<b>Heterogeneous Quasi One Dimensional (He-Qu-1D) model and Ultrasonic Burning Rate (UBR) technique</b>	<b>39</b>
3.1	Heterogeneous Quasi One dimensional (He-Qu-1D) model . . . . .	39
3.1.1	Multi modal AP geometry in propellant . . . . .	40
3.1.2	Pure AP 1D deflagration . . . . .	41
3.1.3	Quasi 1D deflagration of binder matrix coated AP particles . . . . .	43
3.1.4	Effect of burning rate modifiers . . . . .	43
3.2	Ultrasonic burn rate (UBR) technique . . . . .	45
<b>4</b>	<b>Model predictions and experimental data of composite solid propellant compositions</b>	<b>46</b>
4.1	Results and Discussion . . . . .	46
4.2	Comparison of predictions with PSDs from wet and dry method of laser scatter . . . . .	51
<b>5</b>	<b>Conclusion and future work</b>	<b>55</b>
	<b>References</b>	<b>57</b>

# List of Figures

1.1	Schematic of a solid rocket motor . . . . .	7
2.1	Scattering of laser according to the particle size . . . . .	16
2.2	Optical unit of Malvern Mastersizer 3000 . . . . .	17
2.3	Dry dispersion unit . . . . .	18
2.4	Wet dispersion unit . . . . .	19
2.5	Cumulative AP particles size distribution of fine and coarse AP by sieve analysis . . . . .	20
2.6	Optical microscopic image of AP Coarse particles and approximate equivalent circles . . . . .	21
2.7	Image of AP Coarse particles . . . . .	21
2.8	Image of AP Fine particles . . . . .	22
2.9	Image of AP ultrafine particles . . . . .	22
2.10	Particle size distribution of AP from image analysis . . . . .	23
2.11	PSD of AP by wet analysis Laser scatter method . . . . .	23
2.12	Illustration of the dispersion mechanisms in dry method . . . . .	24
2.13	Variation of PSD of AP coarse w.r.t pressure . . . . .	25
2.14	Particle size distribution of coarse-AP at 2 bar and 0.2 bar air pres- sures. . . . .	25
2.15	Particle size distribution of fine-AP at 2 bar and 0.2 bar air pres- sures. . . . .	26
2.16	Particle size distribution of ultrafine-AP at 2 bar and 0.2 bar air pressures. . . . .	26
2.17	Particle size distribution of all the three classes of AP using laser scatter dry method . . . . .	27
2.18	Particle size distribution of ultrafine AP measured after 10 minutes of production at 2.0 bar using laser scatter dry method. . . . .	28

2.19	Comparison of particle size distribution of ultrafine AP using both wet and dry method of laser scatter . . . . .	29
2.20	Change of particle size distribution of ultrafine AP with time after its production . . . . .	30
2.21	Cumulative particle size distribution of AP Coarse . . . . .	31
2.22	Cumulative particle size distribution of AP fine . . . . .	32
2.23	Particle size distribution of AP Coarse comparison with image analysis data . . . . .	32
2.24	Particle size distribution of AP fine comparison with image analysis data . . . . .	33
2.25	Particle size distribution of AP ultra fine comparison with image analysis data . . . . .	33
2.26	A typical report of particle size distribution by Laser scatter . . . . .	35
2.27	Representation of Multi-modal particle size distribution of AP coarse particles . . . . .	36
2.28	Representation of Multi-modal particle size distribution of AP fine particles . . . . .	37
2.29	Representation of Multi-modal particle size distribution of AP ultra-fine particles . . . . .	38
3.1	Pure AP combustion . . . . .	41
3.2	Propellant specimen of UBR bonded in specimen holder. . . . .	45
3.3	Ultrasonic burning rate test set up . . . . .	45
4.1	Prediction and Experimental data of Type 1 propellant composition . . . . .	47
4.2	Prediction and Experimental data of Type 2 propellant composition . . . . .	48
4.3	Prediction and Experimental data of Type 3 propellant composition . . . . .	48
4.4	Prediction and Experimental data of Type 4 propellant composition . . . . .	49
4.5	Prediction and Experimental data of Type 5 propellant composition . . . . .	49
4.6	Prediction and Experimental data of Type 6 propellant composition . . . . .	50
4.7	Predictions and experimental results of Type 3 propellant with and without catalyst. . . . .	50
4.8	Comparison of prediction with PSDs measured by laser scatter wet method and dry method and experimental results of Type 1 propellant . . . . .	51



---

4.9	Comparison of prediction with PSDs measured by laser scatter wet method and dry method and experimental results of Type 2 propellant . . . . .	52
4.10	Comparison of prediction with PSDs measured by laser scatter wet method and dry method and experimental results of Type 4 propellant . . . . .	52
4.11	Comparison of prediction with PSDs measured by laser scatter wet method and dry method and experimental results of Type 5 propellant . . . . .	53
4.12	Comparison of PSD of all classes of AP measured by both Laser scatter wet and dry methods . . . . .	53
4.13	Comparison of master PSD curve of AP by integrating all the classes. . . . .	54

# List of Tables

2.1	Properties of ammonium perchlorate . . . . .	14
2.2	Classification of AP powder based on its particle size distribution . . . . .	14
2.3	Cumulative proportions of each class of AP by seive analysis . . . . .	20
2.4	Parameters for particle size distribution determination using dry method in Malvern Mastersizer 3000 . . . . .	27
2.5	Comparison of different techniques of PSD measurements . . . . .	34
2.6	Parameters of PSD of AP coarse shown in Figure 2.27 . . . . .	36
2.7	Parameters of PSD of AP coarse shown in Figure 2.28 . . . . .	37
2.8	Parameters of PSD of AP coarse shown in Figure 2.29 . . . . .	37
4.1	Different compositions taken for the prediction . . . . .	47

# Chapter 1

## Introduction

Composite solid propellant formulations being used in space launch vehicle applications are majorly based on an oxidizer - ammonium perchlorate (AP) which constitutes from 65-86 % of the total composition, a metallic fuel - aluminium powder of 0-18 %, and a binder - hydroxyl terminated poly butadiene (HTPB) which constitutes of 10-15% of the total composition. Based on the specific ballistic and structural requirements a composition is usually altered and tailoring of the composition is majorly done to obtain the required ballistic behaviour of the propellant, especially the burning rate.

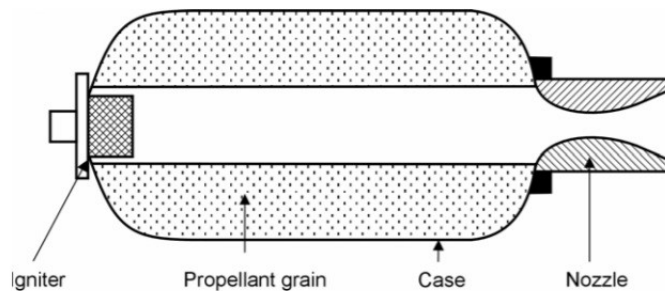


Figure 1.1: Schematic of a solid rocket motor

Hence, achieving a required burning rate for a particular application in a solid rocket motor, Figure 1.1, the solid propellant has to undergo rigorous trials and tests with a set of compositions which is time consuming and cumbersome with a set of compositions. However, with a good and reliable theoretical predictive tool, these tests can be reduced and increase the confidence of the designer. In this context, many burning rate models were developed and are being developed by the solid propellant



community in the world since many decades. To mention a few, Hermance[1, 2], BDP model [3] and Cohen [4, 5] and many others [6, 7, 8, 9, 10] had attempted to model the solid propellant combustion. Nevertheless, none of these models could turn out to be an easy and effective tool for the accurate prediction of the ballistic behaviour of the solid propellant. However, the Heterogeneous Quasi 1-D model[11, 10, 12] developed based on the physical aspects of solid propellant combustion which is governed by the particle size distribution of the oxidizer i.e., AP, appears producing promising results. This model has been developed based on the serial burning approach adopted from studies of previous investigators [13, 5]. The model requires accurate distribution of particle size of AP. Hence major emphasis was given in this present work to develop a methodology of accurate measurement of AP particle size distribution (PSD). Knowing particle size distribution, the burning rate of the several compositions of propellant based on AP/HTPB/Al /Catalysts are predicted using the model and the results are compared with the actual burning rates of these propellants measured by ultrasonic technique (UBR).

Based on the particle size distribution, AP grains are classified into three categories viz. coarse, fine and ultrafine. Different techniques were explored for the measurement of AP particle size distribution of all the three classes and an easy and accurate method of measuring the particle size distribution is evolved.

## 1.1 Literature review

### 1.1.1 Particle size distribution of Ammonium Perchlorate

Though particle size distribution of AP is having such significance in the burning rate of solid propellant, very little work had been pursued to standardize the accurate measurement of particle size distribution of AP. Conventionally sieve analysis has been the measurement technique for the solid propellant community while processing the propellant. There are numerous techniques of evaluation of particle size distribution. Selection of appropriate technique for a particular material depends of many factors. However, investigators or plant quality engineers expect to get the results as fast as possible and hence time is one of the crucial factors of consideration, but not in lieu of accuracy and reproducibility. Kelly and Etzler[14] in their publication had

discussed the laser diffraction technique of measurement of particle size distribution, in particular non spherical particles and had specified a good understanding on selection of right method of measurement of PSD . Although they advocates for an urgent review of these techniques in use, the process of selection which they have discussed i.e., comparison of any technique with microscopic analysis is a good strategy to be followed.

Li et.al [15] investigated on the measurement of PSD using different techniques viz., Laser diffraction (LD) , image analysis (IA) , ultrasonic attenuation spectroscopy (UAS) , focused beam reflectance measurement (FBRM) . Their study was majorly on the materials which are non-hygroscopic and hence the effect of agglomeration due to moisture was not accounted. For spheres, the PSDs obtained by image analysis, laser diffraction and ultrasonic attenuation spectroscopy are in good agreement. It is shown that particle shape strongly affects the PSDs measured by different techniques for non-spherical particles. There is no consistent PSD result from different particle measurement techniques due to the influence of shape. correlation among particle size distributions by these three techniques is possible[15] and can be done using the particle shape factors obtained by IA. Chord 50 corresponds to FBRM measurement technique.

For spherical particles,

$$D_{50LA} \approx D_{50LD} \approx D_{50UAS} > Chord_{50} \quad (1.1)$$

For non-spherical particles,

$$D_{50LA} > D_{50LD} > D_{50UAS} \text{ or } Chord_{50} \quad (1.2)$$

where  $D_{50}$  represents the value below which 50% by volume of the particles exists in the sample.

Miller [8] has studied on the effect of size of the AP on propellant burning rate. He also reiterates that burning rate increases with decrease of particle size. The particle size distribution measurement of AP was carried out by screening using standard sieves for coarser particles and electrozone celloscope analysis [16] was employed for finer particles. Ultrafine particles were analysed by sedimentation technique. Here also, the validation of these techniques of particle size distribution measurement was

done with microscopic data.

Jain et. al. [17] carried out investigation on effect of PSD on burning rate and propellant slurry viscosity. Major emphasis was given on the shape of the particle and its influence on propellant mixing and burning rate. As far as size of the particle is concerned, only the average particle is taken into account and not the size distribution and span, thus considering a mono-modal distribution of AP particles. It is also reported about the shape factor which indicates that the sphericity of the particles is higher for the coarser particles

Eshel et. al.[18] had carried out a detailed study on laser diffraction method of measurement of particle size distribution. The material of interest of their study was soil. However, their attempts to compare the PSD by sieve, sedimentation and laser diffraction techniques were not successful and there was no good agreement between the results from these techniques. Neither they could establish a correlation between these techniques. But, in this study, they have shown that refractive index has effect on the measurement of PSD by laser diffraction technique.

Jeenu et. al. [19] measured the particle size distribution of condensed particles in the combustion products of aluminized composite solid propellant. They had used laser diffraction technique to measure the PSD. This work by Jeenu et. al. [19] shows a representation of PSD data fitted into a multimodal log normal distribution. This will be discussed in detail in the later chapters of this article as this method of representation is adopted for the present work also.

### **1.1.2 Modelling of combustion of composite solid propellant and its prediction of ballistic behaviour**

Many models of solid propellant combustion and prediction of burning rate has been proposed and developed by many investigators for many decades. It is well accepted that burning rate of solid propellant is a function of pressure, oxidizer to fuel (O/F) ratio, oxidizer particle size distribution and type and percentage of additives (catalysts). As the name implies composite solid propellant is heterogeneous in nature and hence heterogeneity of composite solid propellant is one aspect which need to be taken into



account. Hermance [1] has developed a model taking heterogeneity in the condensed phase of solid propellant and heat generation taken in to account. Hermance[1] has considered this three-dimension unsteady phenomenon and converted into a one dimensional steady state in his model. Further, it has been modified [2] with inclusion of diffusional mixing process in the determination of flame standoff distance.

Backstead et. al. [13, 3] had introduced a model which states that heat release in the gas phase is contributed by three flames 1) primary diffusion flame between the decomposition products of binder and oxidizer, 2) mono propellant(oxidizer) premixed flame, 3) final diffusion flame between the primary decomposition products of mono propellants and products of premixed flame. Further many scientists modified these models and were elegant at their inception. But these models were somehow not been used by the designer who could readily develop a composition with the desired ballistic behaviour with the confidence of the theory proposed by these models due to complexity of the model and may be lack of confidence in the models itself.

Recently Gross and co investigators[20, 21, 7] has come up with a tool to model the combustion process and predict the burning rate of composite solid propellant. Here the burning rates were calculated by numerical simulations of CFD which requires time and high computational resources.

## 1.2 Outline of the thesis

The next chapter explains in detail about the ammonium perchlorate and its particle size distribution. A detailed analysis of particle size distribution of AP using different measurement techniques and their comparison. Advantages and disadvantages of each technique is discussed

The third chapter describes in brief the heterogeneous quasi one dimensional burn rate prediction model and its the novel technique of experimental measurement of burning rate of solid propellant i.e., Ultrasonic Burning Rate (UBR).

The fourth chapter deals with the predictions of different solid propellant compo-

sitions with dry method of particle size distribution of AP and comparison of the burning rate results with experimental results generated with UBR.

The fifth chapter is for conclusion and the proposal of the future work to make this model further robust.

# Chapter 2

## Ammonium Perchlorate and its particle size characterization

### 2.1 Ammonium Perchlorate

Ammonium Perchlorate (AP) is a white, crystalline solid with chemical formula  $\text{NH}_4\text{ClO}_4$  (see Table 2.1) is generally used as oxidizer in almost all the solid propellant formulations of ISRO. Most of the composite solid propellant compositions contain solid loading up to 86% of AP thus making it the main solid ingredient of composite solid propellant. Moreover, due to the high available oxygen content and high density. It secures its position as workhorse oxidizer in solid propellant. Other main ingredients are aluminium powder and hydroxyl terminated polybutadiene (HTPB) which acts as a fuel-cum-binder material for AP and aluminium powder particles. The two most important ballistic properties of solid propellant are its energy content (heat of combustion) and burning rate. The energy content is determined by the composition whereas the burning rate is not only a function of composition, but is a strong function of particle size distribution (PSD) of ammonium perchlorate(AP). Hence, it is very important to know the size distribution of AP particles that goes into the propellant composition. Usually, AP powders with different particles size distributions are added to propellant in order to control the burning rate and increase the AP solid loading in the propellant. Based on the average particle size distribution, they can be called as coarse, fine, and ultrafine AP (Table 2.2). These three classes of AP powers are added in different proportions in order to get the required burning rate to the propellant. In addition, these proportions controls the viscosity of the propellant slurry and the mechanical properties of cured propellant.

Chemical formula	$\text{NH}_4\text{ClO}_4$
Molar mass	117.49 g/mol
Appearance	White crystalline
Density	1.95 g/cm <sup>3</sup>
Melting point	Exothermic decomposition before melting above 200°C
Solubility in water	20.85 g/100 ml (20°C)
Solubility	Soluble in Methanol and water, partially soluble in acetone and insoluble in ethyl acetate and ether.

Table 2.1: Properties of ammonium perchlorate

Class	Particle size range (microns)	Production method
Coarse	500 – 150	Prepared by crystallization and sieving. Crystallization conditions affects the distribution
Fine	150 – 20	Prepared by grinding in an attrition mill or hammer mill. Feed rate control the distribution.
Ultra fine	less than 20	Prepared by grinding in fluid energy mill. Clustering may happen on storage.

Table 2.2: Classification of AP powder based on its particle size distribution

## 2.2 Particle size distribution

As the particle size distribution of AP is a very important measurement to characterize the propellant, it is very much essential to measure it accurately. The particle-size distribution can be defined as distribution of the relative amount, typically number, mass or volume of particles present in a sample according to the particle size. Over the period of time, many techniques had evolved for the accurate measurement of particle size distribution. In the current work, the following techniques were used for the measurement

- Sieve analysis
- Microscopic method and image analysis

- Laser scatter: dry method and
- Laser scatter: wet method

### 2.2.1 Sieve analysis

This method is a standard measurement technique conventionally being used in ISRO for the measurement of particle size distribution of AP. A set of standard sieves of known mesh sizes arranged progressively from larger mesh at the top to smaller mesh at the bottom in a sieve shaker. A known amount of powder material is added at the top. After a fixed time of shaking, the particles retained in each sieve is weighed and mass distribution is obtained. A large amount of materials can be readily loaded into sieve trays to improve the measurement accuracy. As far as AP is concerned, being a hygroscopic material there is an uncertainty with finer particles. These particles may get adhered to the sieve. These cases make the sieve analysis inferior method of measuring particle size distribution especially for AP.

### 2.2.2 Microscopic method and image analysis

This method is more accurate as the actual dimensions of particles can be directly measured with the help of a microscope. Size of all particles can be noted, but for a statistically valid analysis, very large number ( $>1000$ ) of particles have to be measured. This is time consuming and cumbersome. However, automated image analyzing techniques are now available to obtain an accurate particle size distribution. The main difficulty with this technique is the preparation of a well and representative spread of particle on the slide of the microscope. It is extremely difficult to measure for very fine particles due to clustering.

### 2.2.3 Laser scatter method

In this method, the particles disperse in a medium in a measurement cell are illuminated in a collimated laser beam, causing the light to be scattered in different directions. Bigger particles will bring about a high intensity of scattering at low angles to the beam. Smaller particles, on the other hand, create a low intensity signal at far wider angles as shown in Figure 2.1. The intensity of scattered light at various angles are measured with specially-designed ring shaped annular detectors and particle size distribution is determined from the resulting data.

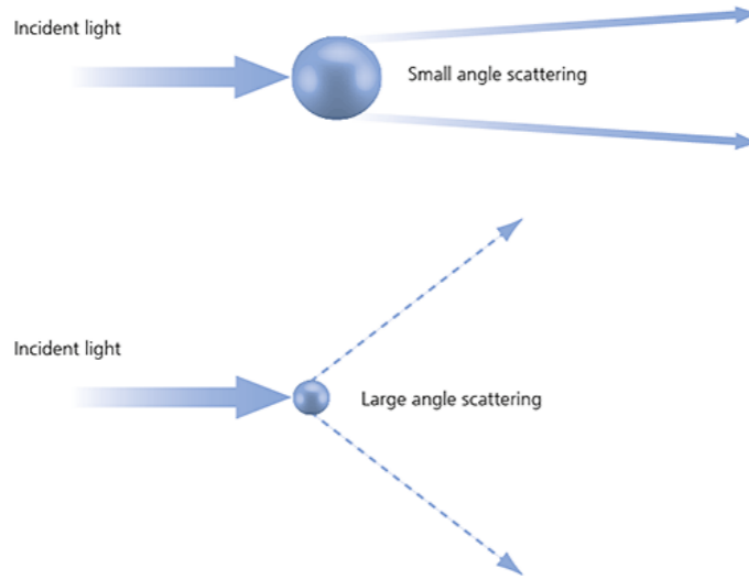


Figure 2.1: Scattering of laser according to the particle size

Different dispersion medium can be used for dispersing the particles. In dry method, the dispersion medium is dry air which carries the particles through an optical measurement cell. In wet method, the sample is dispersed in liquid and circulated through the optical measurement cell. For AP particles, the suggested liquids are ethyl acetate or n-butyl acetate for wet method of dispersion.

## 2.3 Laser diffraction particle size analyser

The laser diffraction particle size analyser (Malvern Mastersizer 3000) employing laser scatter technique available at Rocket Propellant Plant(RPP) in Vikram Sarabhai Space Centre (VSSC) is used for the measurement of particle size of AP powder. This equipment is capable of measuring particle size distribution in the range of 0.1 to 3000  $\mu\text{m}$ . The Malvern Mastersizer is comprised of a main optical unit, one or more dispersion units and a measurement cell as shown in the Figure 2.2 .

The optical unit transmits red and blue laser light through a well dispersed powder sample and uses light detectors to generate data from the light scattering pattern caused by the particles in the optical cell. The data is then interpreted by the Mastersizer application software to provide the particle size information. The blue laser light improves the measurement resolution for particles below  $1\mu\text{m}$  size.



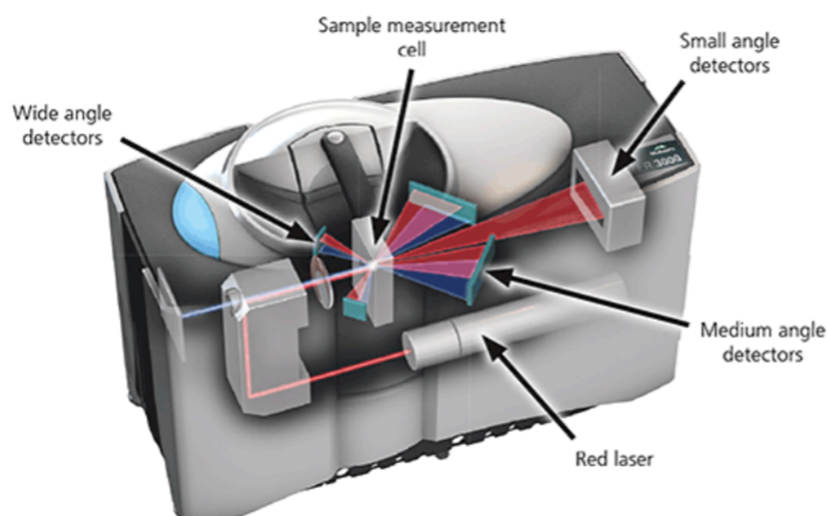


Figure 2.2: Optical unit of Malvern Mastersizer 3000

### 2.3.1 Dry method

The dry powder sample is manually placed in the sample hopper fitted to the top of the vibrating sample feed tray of the dispersion unit as shown in the Figure 2.3. Additionally, a mesh basket with a steel ball, is used to help smooth the flow of sample and break up any loose agglomerates within the sample before it falls into the venturi disperser. The air supply and vacuum suction system is connected. When the sample feed tray vibrates the sample in the hopper travels down the tray until it eventually falls into the main feed mechanism - the venturi disperser.

The rate at which the sample is fed into the venturi disperser is governed by the amplitude of vibration of the feed tray (controlled by the software) and also by the gap set between the feed tray and hopper on the sample tray. As the sample falls through into the funnel of the venturi disperser, it is accelerated by compressed air within the centre of the venturi disperser where agglomerates are dispersed. The sample is then directed through the dry measurement cell fitted to the Mastersizer optical unit, where it is measured and then collected by the vacuum suction system at the rear of the dry cell.

### 2.3.2 Wet method

The wet (Hydro EV) dispersion unit uses a 600 ml or one litre glass beaker to hold the sample and dispersant liquid. This dispersion unit consists of a pump head which

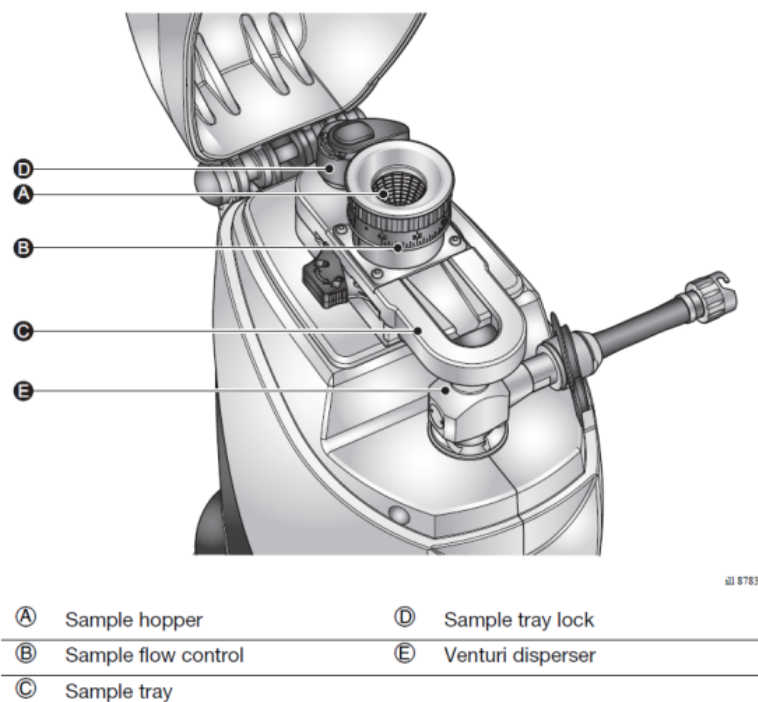


Figure 2.3: Dry dispersion unit

can be tilted. This pump head will be immersed into the dispersant as shown in Figure 2.4. The pump-head is tilted forward, lowering the pump arm into the beaker, and allowing the dispersant to be pumped. The pump circulates the dispersant from the dispersion unit to the wet cell located in the optical bench, via the sample tubing and the pumping speed is controlled by the Mastersizer application software. Sample is then added to the beaker as required. The stirrer agitates the sample to prevent settling the particles. An ultrasonic transducer is provided to aid the dispersion of the powder and also to remove bubbles from the flow path.

## 2.4 Particle size analysis using different techniques and results

Measurement of particle size distribution of AP was carried out using all the above discussed techniques. All the three classes of AP had been analysed with different techniques. The laser scatter dry method being a new technique of dispersing the sample, the parameters for accurate measurement has been worked out and is discussed in further sections of this report. The below are the results for each technique.

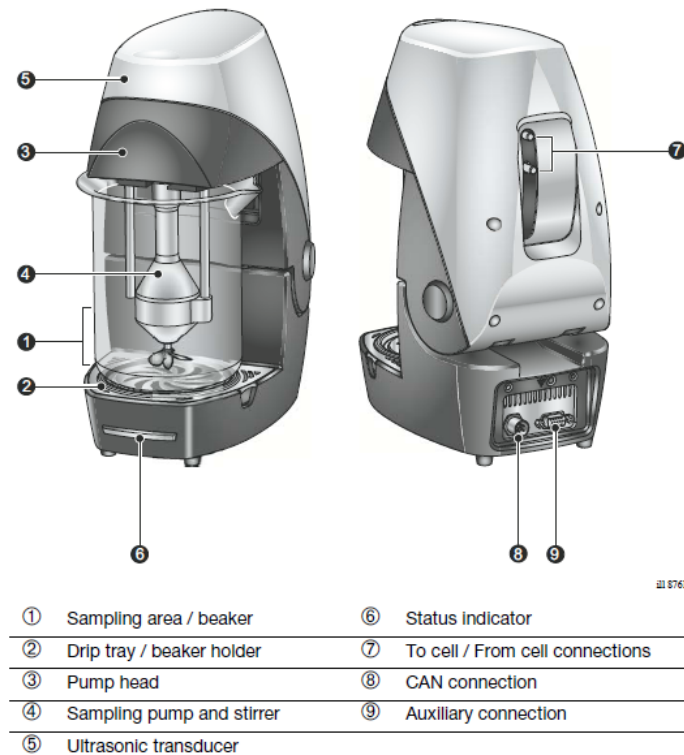


Figure 2.4: Wet dispersion unit

### 2.4.1 Sieve analysis

In the sieve analysis, the measurements depend on the available standard sieves for a range of AP particle sizes. For the AP-coarse and AP-fine classes of particles the cumulative mass density distributions are shown in Figure 2.5. The cumulative proportions of each class is given in table 2.3 as there is no availability of necessary sieves for the ultrafine AP, it could not be analysed by this technique.

### 2.4.2 Microscopic method

The Malvern make particle shape analyser was used for obtaining the particle size analysis by microscopic method. The equipment analyses the image of the particle (projected area of the particles image) from which the particle size distribution is obtained by counting. The analysis gives the number distribution against particles diameter. Hence, it has been converted to volume density for comparison. The microscopic image of the AP coarse particles is shown in Figure 2.6.

The images of the individual AP coarse, fine and ultrafine particles obtained from Malvern shape analyser is also shown in figures 2.7, 2.8 and 2.9.

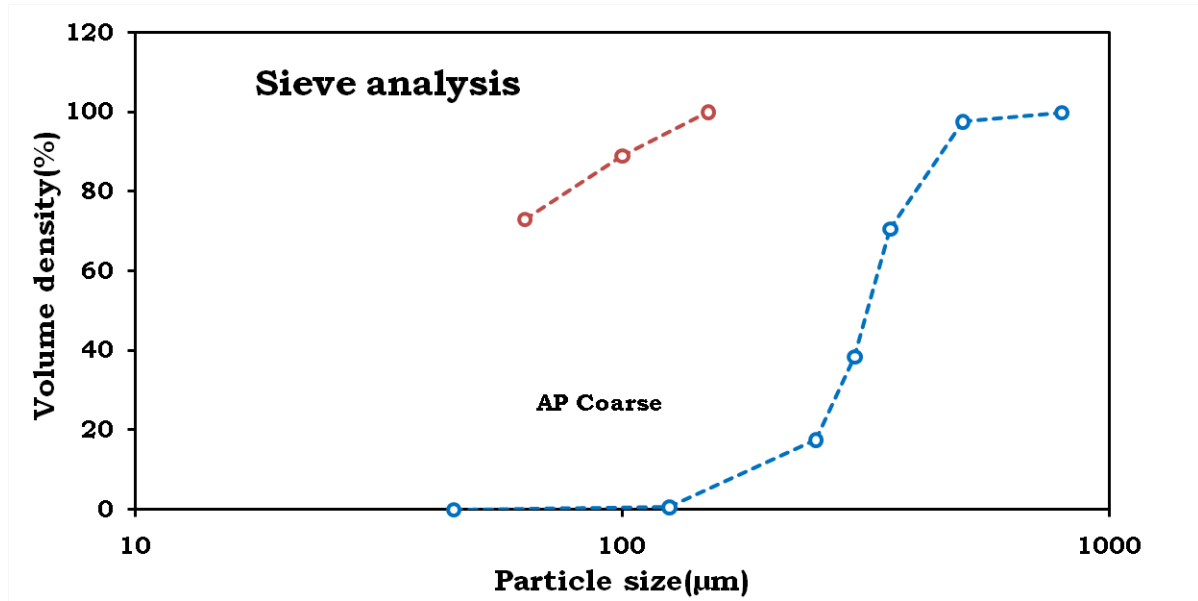


Figure 2.5: Cumulative AP particles size distribution of fine and coarse AP by sieve analysis

AP coarse		AP Fine	
Particle size ( $\mu\text{m}$ )	Cumulative volume density (%)	Particle size ( $\mu\text{m}$ )	Cumulative volume density (%)
45	0.01	63	73
125	0.6	100	89
250	17.56	150	100
300	38.43		
355	70.61		
500	97.53		
800	99.91		

Table 2.3: Cumulative proportions of each class of AP by sieve analysis

It is observed that the AP coarse particles have a shape of two or more particles fused together. This shape might have occurred during its crystallization process. AP fine and AP ultrafine particles do not show the above said characteristic, but could detect particles with sharp corners. The particle size distributions measured by optical analysis are shown in Figure 2.10.

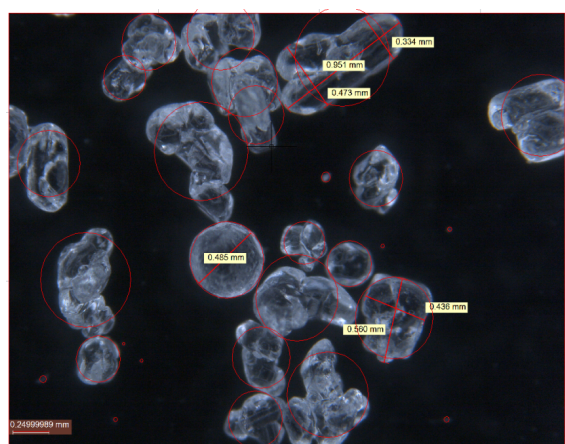


Figure 2.6: Optical microscopic image of AP Coarse particles and approximate equivalent circles

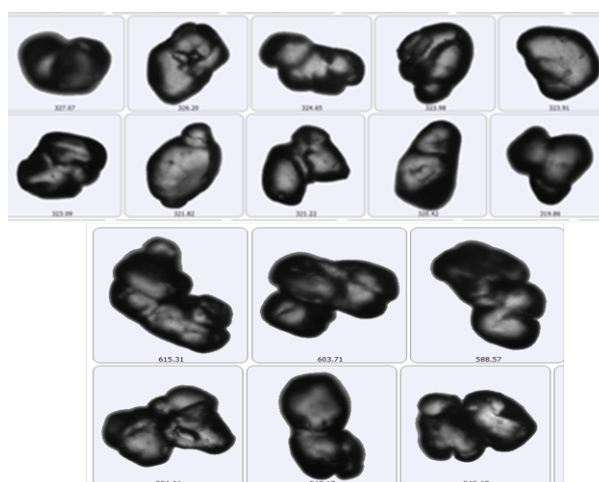


Figure 2.7: Image of AP Coarse particles

### 2.4.3 Laser scatter - Wet analysis

Particle size distribution of AP using laser scatter wet method was carried out using Malvern Mastersizer 3000. Here the carrier medium to circulate through the measurement cell was ethyl acetate or n-butyl acetate for AP particles. It is a well-established method for the measurement of particle size distribution of powders in Analytical and Spectroscopy Division(ASD), VSSC . This method of analysis is appropriate for hard particles such as powders of metals or oxides which will not disintegrate further during agitation and circulation through the cell and will not dissolve in the solvent or liquid in which the particles are dispersed. In the case of AP, being a crystalline salt and comparatively soft, the crystals may further break during dispersion and absolute

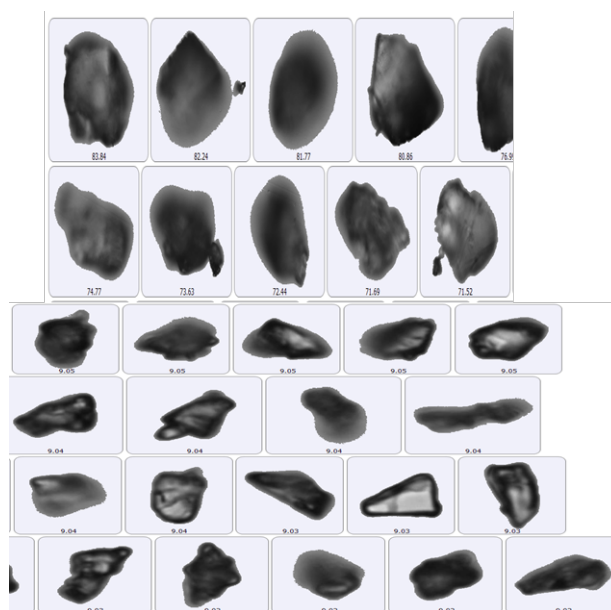


Figure 2.8: Image of AP Fine particles

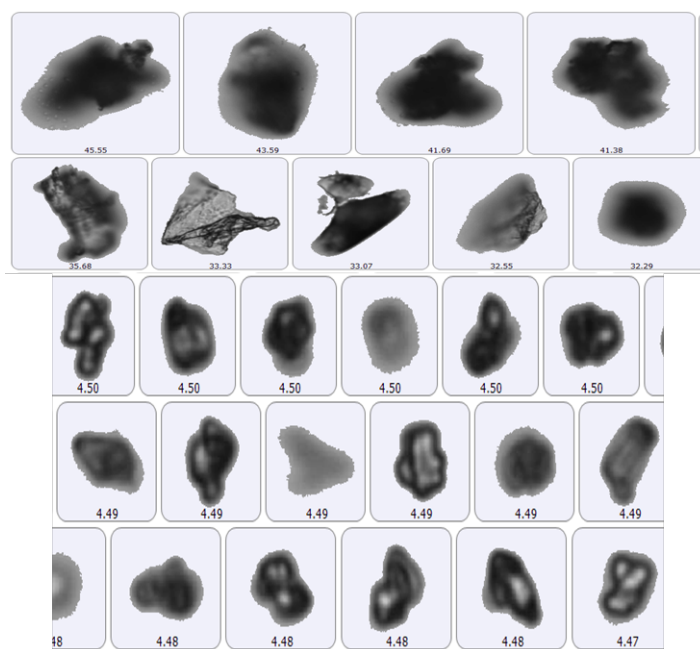


Figure 2.9: Image of AP ultrafine particles

insolubility is not claimed in any of the solvents. Instead, we choose to analyse in a solvent in which AP is nearly insoluble. This uncertainty in measurement is a real concern and has to be addressed for an accurate measurement of particle size distribution. The particle size distribution of different classes of AP using laser scatter wet method is shown in Figure 2.11

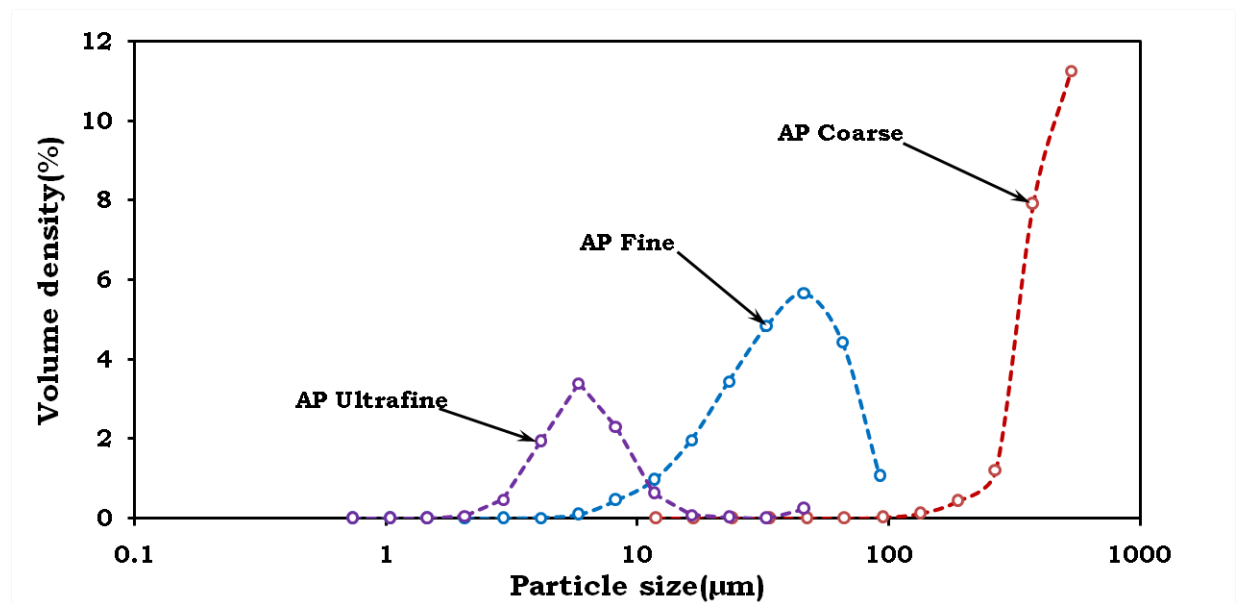


Figure 2.10: Particle size distribution of AP from image analysis

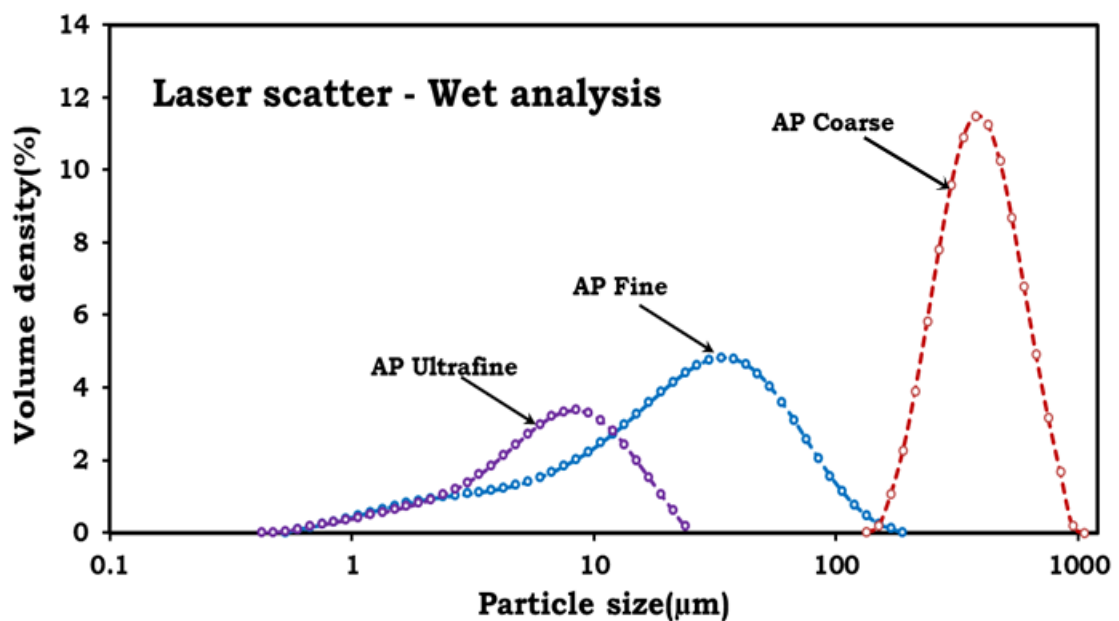


Figure 2.11: PSD of AP by wet analysis Laser scatter method

#### Laser scatter - Dry analysis

In dry analysis, the carrier of the sample to the measurement cell is compressed air. As discussed in section 2.3.1, the sample is fed into the sample tray and passed through the venturi-disperser, and then carried away by the air current. There are



few parameters to be optimized for the measurement of AP particle size distribution accurately as this is a new method of dispersion especially for a sample like AP. The feed rate is fixed by optimizing the frequency and amplitude of the vibration of the feed tray and the gap between hopper and tray (hopper gap, which acts as the gate for the sample into the venturi-disperser) and the pressure of the inlet air, which influences the flow of the particles and residency period of the particles in the measurement cell. The sample fed in the dry dispersion method is a once through pass system and the quantity of sample size in a single test is limited due to be constraint of volume of the hopper. Since the period of measurement is fixed, higher the feed rate lower the number of measurements. In view of this, 20% of the vibration amplitude of the tray has been chosen as to maintain the feed rate optimally and number of readings can be maximized for  $\approx 30\text{g}$  of AP sample powder.

It is observed that the optimized hopper gap is 1mm as the AP coarse particles may range from 1 to 700  $\mu\text{m}$ . Further reduction in hopper gap results in the particles to clog inside the hopper and further increase lead to higher feed rate resulting in less number of measurements per test.

The dispersion mechanisms of AP particles in dry method is illustrated in Figure 2.12. It indicates the velocity of particles is an important parameter in dispersing the particles, which in turn determined by the pressure of the feed air. At high pressures, as AP particles are brittle in nature, the particle may break and at low pressures, the dispersion may not be effective. This will affect the particle size distribution. Hence, to get an optimum pressure, the AP was analysed using dry dispersion unit at different pressures ranging from 0.1 bar to 3 bar of air pressure. The results are shown in Figure 2.13.

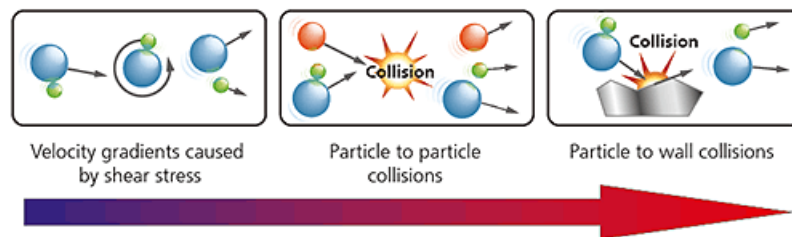


Figure 2.12: Illustration of the dispersion mechanisms in dry method

In the Figure 2.13,  $D_{v10}$ ,  $D_{v50}$  and  $D_{v90}$  are the parameters based on the cumulative particle size data of a given sample. Here  $D_{v10}$ ,  $D_{v50}$  and  $D_{v90}$  denote the maximum particle size ( $\mu\text{m}$ ) below which 10%, 50% and 90% of the sample volume respectively

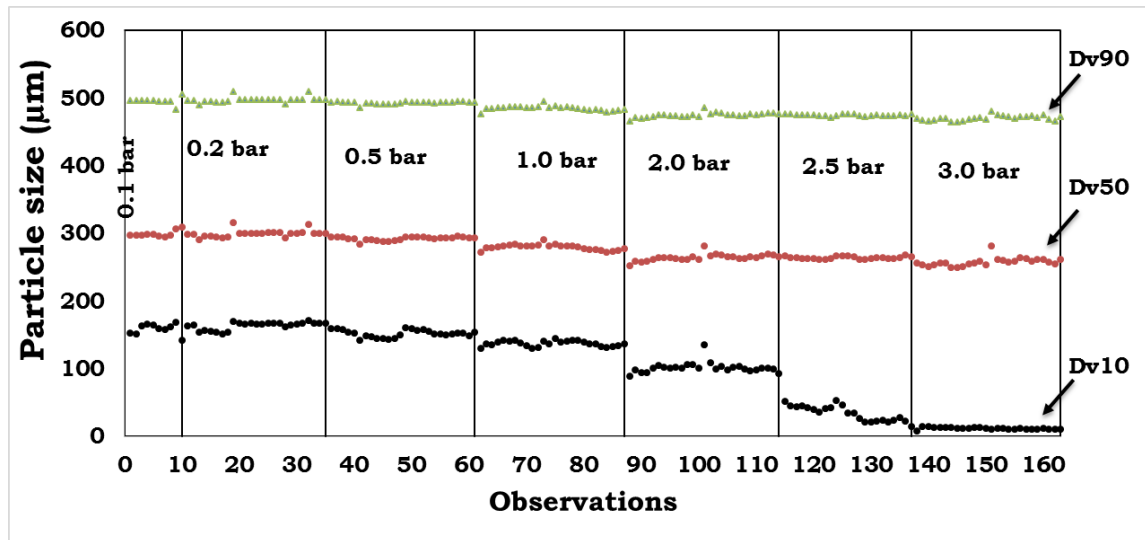


Figure 2.13: Variation of PSD of AP coarse w.r.t pressure

exists. From the Figure 2.13 it is observed that Dv10, which indicated the size of finer particles in the sample below which 10% of the sample volume exists, is smaller if the feed pressures is higher than 1 bar. This is an indication of possible breaking of particles at higher pressures. At lower pressures, Dv10 is found to be constant. Hence a lower pressure, say 0.2 bar, is chosen for the analysis.

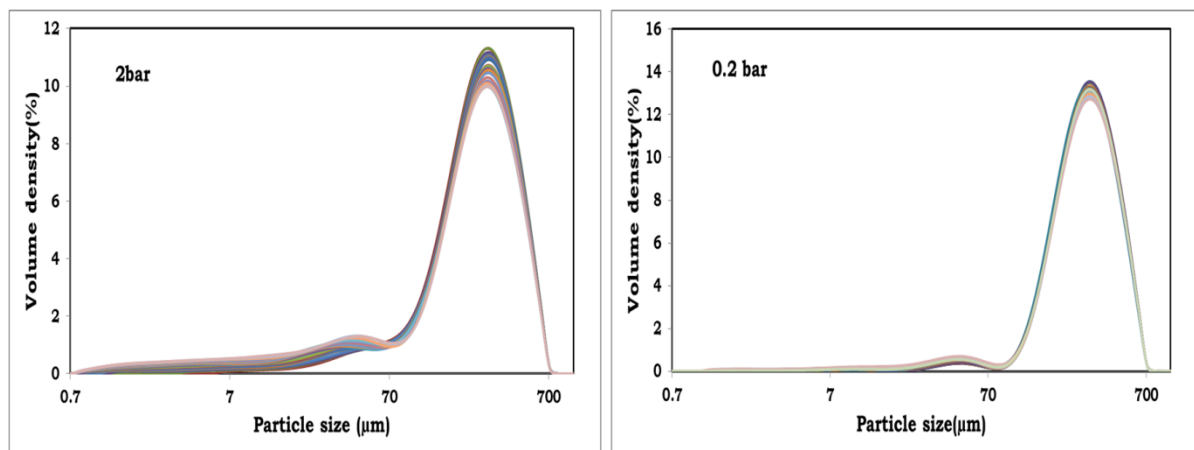


Figure 2.14: Particle size distribution of coarse-AP at 2 bar and 0.2 bar air pressures.

The Figure 2.14 are results of repeated measurements of the same batch of AP coarse sample at 2 and 0.2 bar air pressures. From this, it is clear that the 0.2 bar pressure of air current gives less dispersed results in repeated measurements as compared to 2.0 bar results. It is also evident that the fine particles are increased in 2bar test.

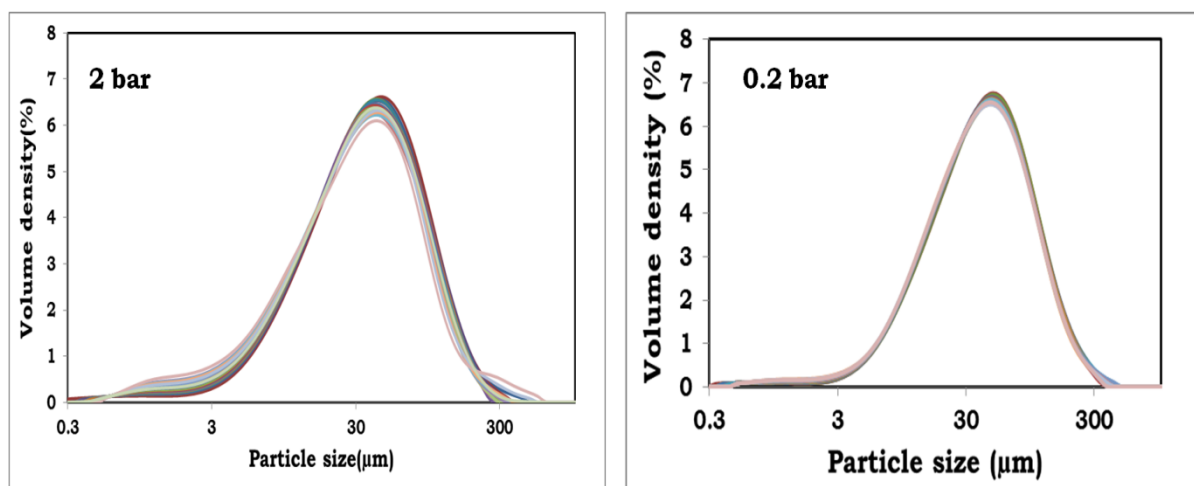


Figure 2.15: Particle size distribution of fine-AP at 2 bar and 0.2 bar air pressures.

Similarly, from the Figure 2.15 which shows the particle size distribution of AP fine at two different pressures and less dispersed results are obtained at lower pressures. However, for ultra fine AP, (see Figure 2.16), as the chances of further reduction of particle size is not easy due to the inter particle and wall collision, it is proposed to use higher pressures i.e., 2 bar. As clustering can occur easily in ultrafine AP, higher pressure is beneficial for the breakage of these clusters. The volume density of ultrafine particles is increased in 2 bar as compared to 0.2 bar which is an indication of agglomeration being dispersed.

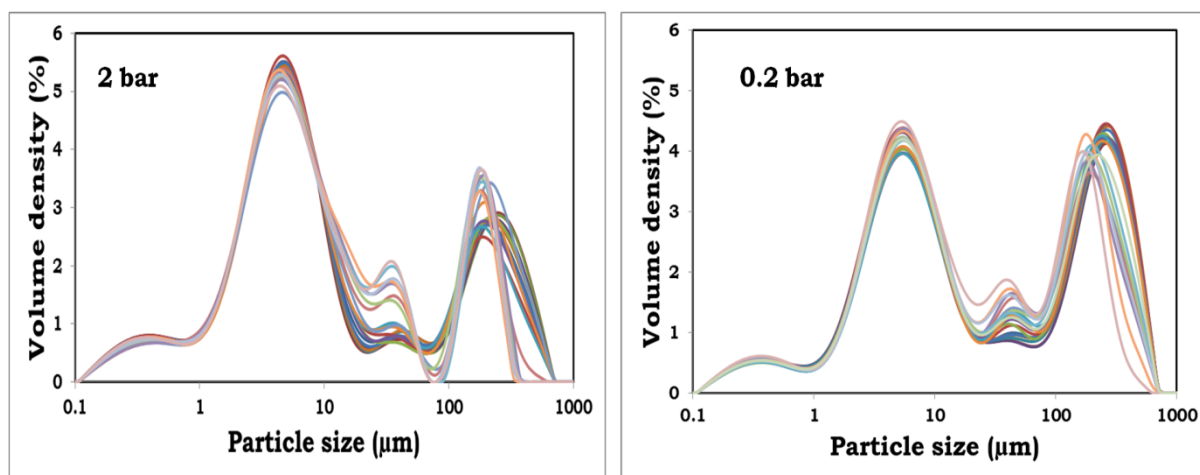


Figure 2.16: Particle size distribution of ultrafine-AP at 2 bar and 0.2 bar air pressures.

Figure 2.17 shows the particle size distribution of all the three classes measured by laser scatter dry method. Based on this study, the parameters shown in Table 2.4

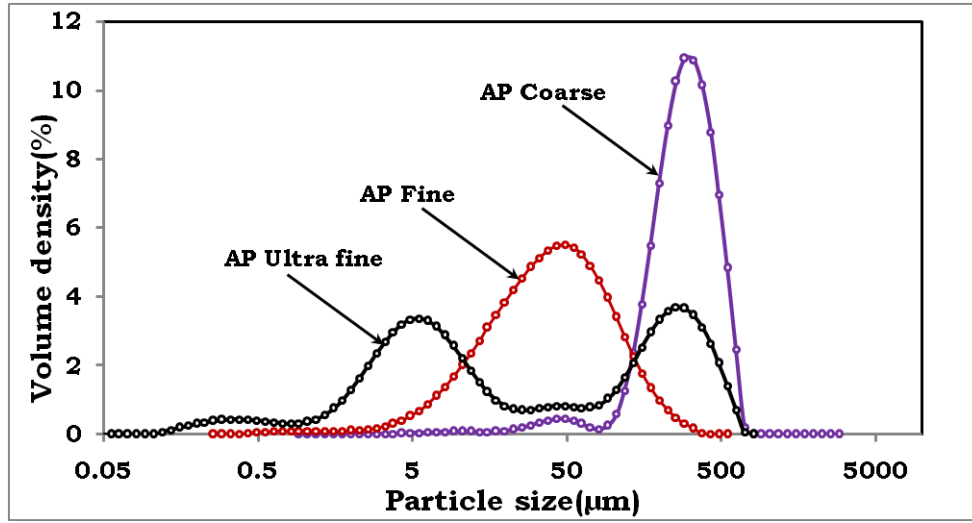


Figure 2.17: Particle size distribution of all the three classes of AP using laser scatter dry method

have been arrived at for the measurement of particle size distribution for all the three classes of AP.

Sl. No.	Parameter	AP coarse	AP fine	AP ultrafine
1	Gap between hopper and sample tray	1mm	1mm	1mm
2	Feed rate	20%	50%	50%
3	Compressed air pressure	0.2 bar	0.2 bar	2 bar
4	Observation time per reading	6 seconds	6 seconds	6 seconds
5	No. of measurements per sample	12	12	12
6	No. of samples per batch	3	3	3

Table 2.4: Parameters for particle size distribution determination using dry method in Malvern Mastersizer 3000

To account for the effect of agglomeration in ultrafine powder of AP, further studies were carried out to understand the effect of time on the agglomeration. If the measurement can be done within 10 minutes of the production of ultrafine powder, we get a particle size distribution with particle size not exceeding 40 microns as shown in Figure 2.18. On the other hand, at lower pressure say 0.2 bar (2.16) we observe a peak showing the agglomerated ultrafine particles which could not be dispersed at 0.2 bar.

A comparison of particle size distribution of ultrafine AP measured by both wet and

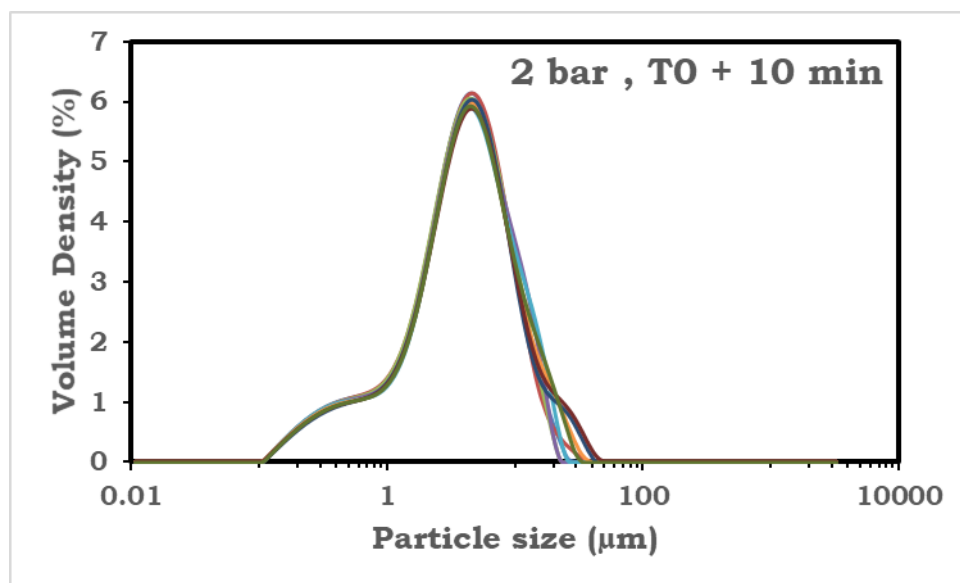


Figure 2.18: Particle size distribution of ultrafine AP measured after 10 minutes of production at 2.0 bar using laser scatter dry method.

dry methods of laser scatter is shown in Figure 2.19. A review into this comparison reveals that in dry method there is higher fraction of very fine particles in the distribution as compared to wet method where this fraction of very fine particles is not observed in measurement. This can be attributed to the dissolution of these very fine particles in ultrafine powder in the solvent while stirring and sonication. The rate of agglomeration is captured in dry method which is indicative in Figure 2.20.

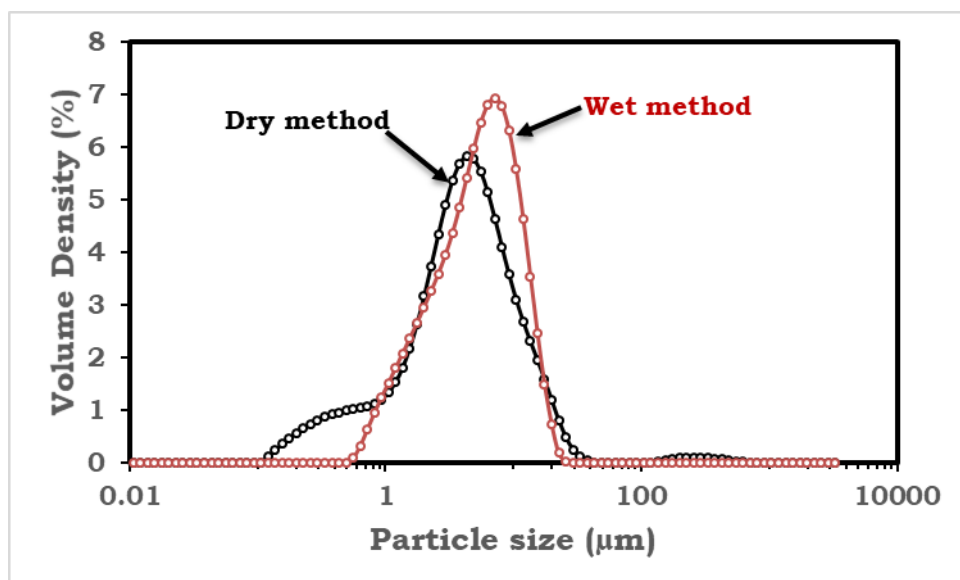


Figure 2.19: Comparison of particle size distribution of ultrafine AP using both wet and dry method of laser scatter

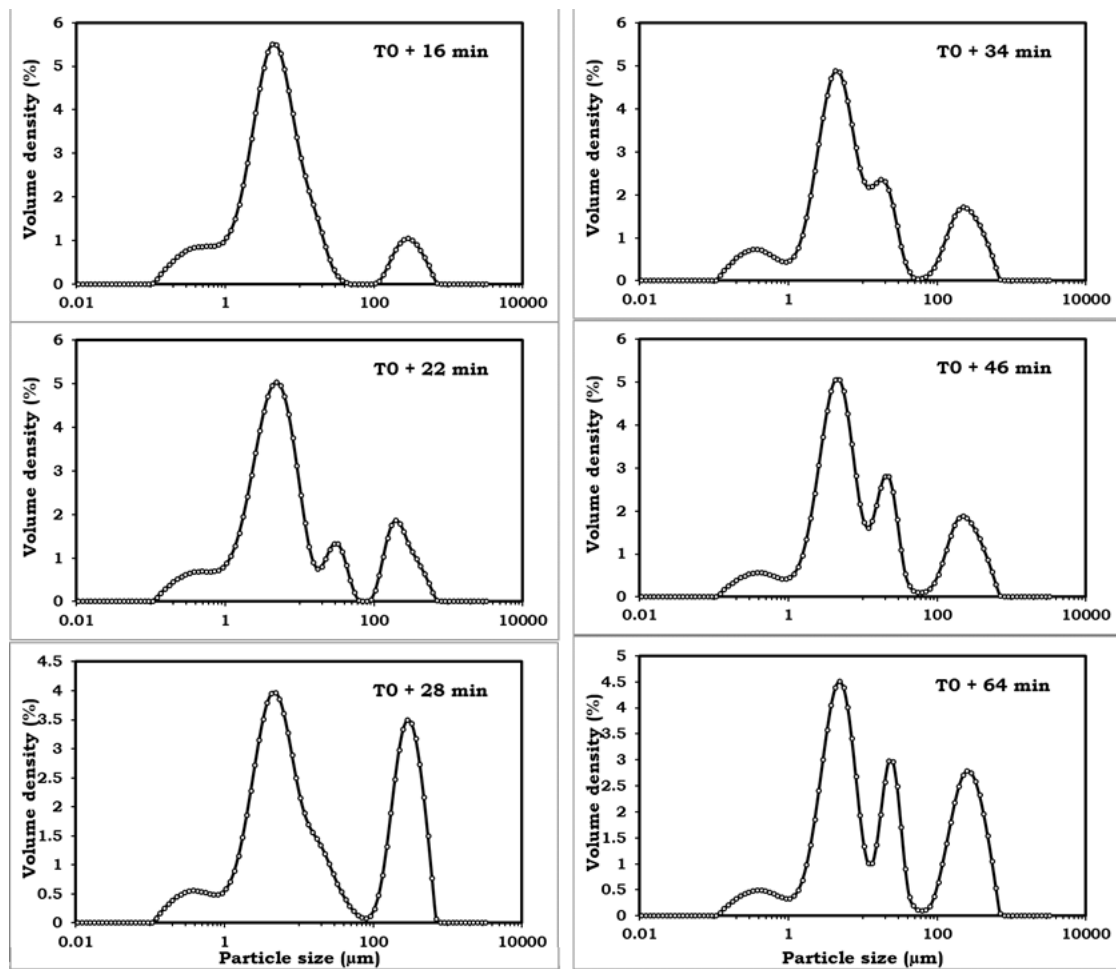


Figure 2.20: Change of particle size distribution of ultrafine AP with time after its production



## 2.5 Comparison of Particle size distribution analysed by different techniques

### 2.5.1 Sieve analysis and laser diffraction techniques

Typical cumulative particle size distribution of AP coarse is shown in Figure 2.21. It is observed that the distribution of AP coarse using sieve analysis is in between the laser scatter techniques of wet and dry methods. For the particles of size above 350  $\mu\text{m}$  the sieve data is in very close agreement with laser scatter dry method. However, dry method measures approximately 5% of fine particles below 100  $\mu\text{m}$  in the coarse AP. This was not detected by either sieve analysis or laser scatter wet method.

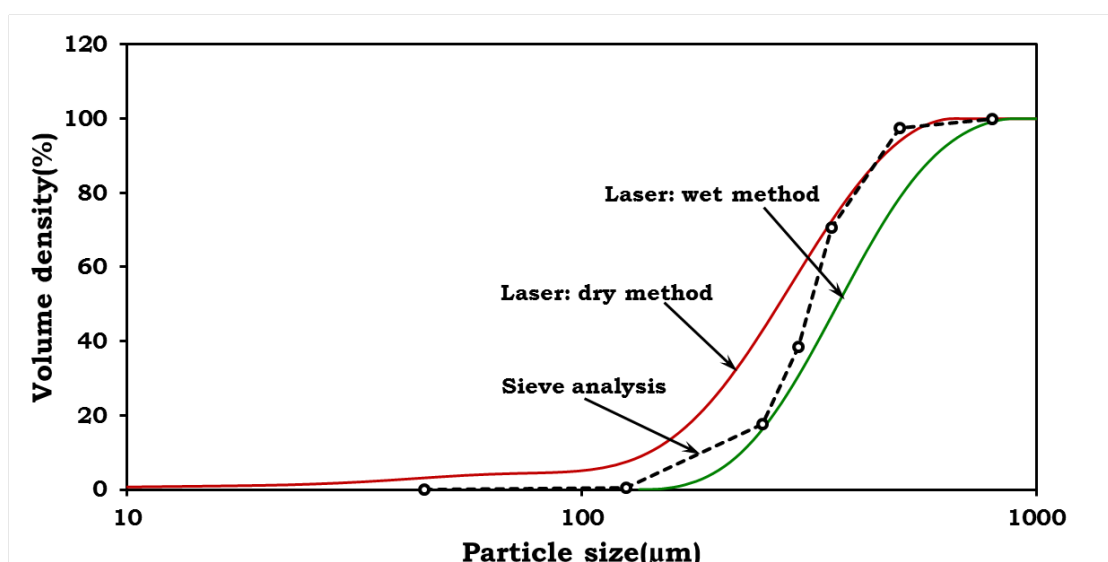


Figure 2.21: Cumulative particle size distribution of AP Coarse

Similarly, Figure 2.22 shows the cumulative particle size distribution of AP fine. The wet method shows larger quantity of finer particles in the fine-AP powder than that by dry method. This may be due to the possibility of particle disintegration during agitation in the mixing container. In sieve analysis of AP fine particles, by virtue of its moisture sensitivity, the particles get adhered to the sieve. And hence, three sieves could only be used in sieving. However, the results are in line with laser scatter dry method.

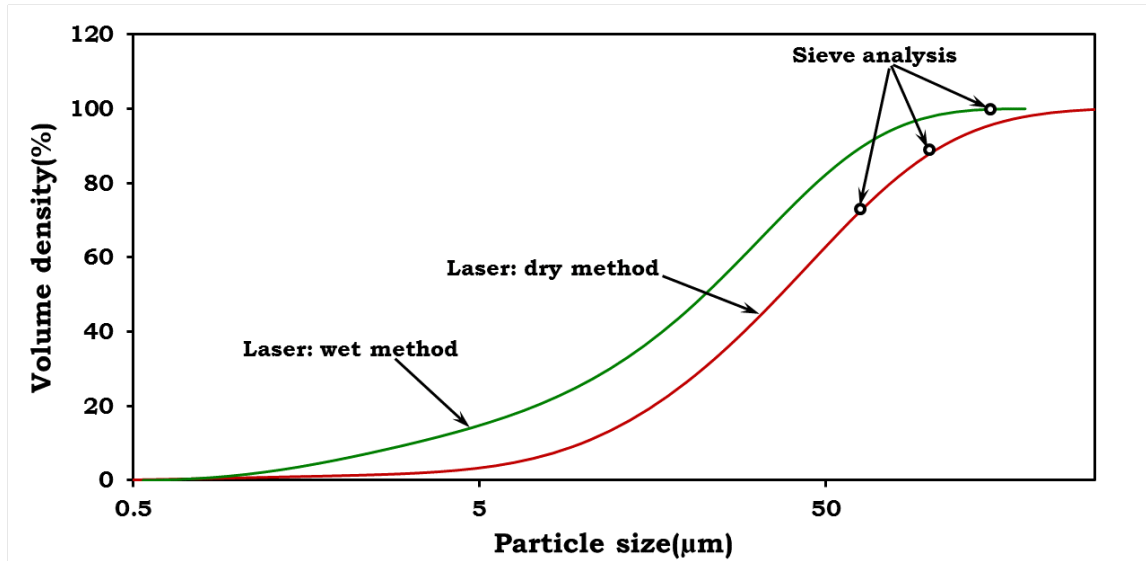


Figure 2.22: Cumulative particle size distribution of AP fine

### 2.5.2 Microscopic (image analysis) and Laser scatter techniques

Figure 2.7 shows the comparison of particle size distribution of AP coarse measured by Laser scatter and microscopic analysis techniques.

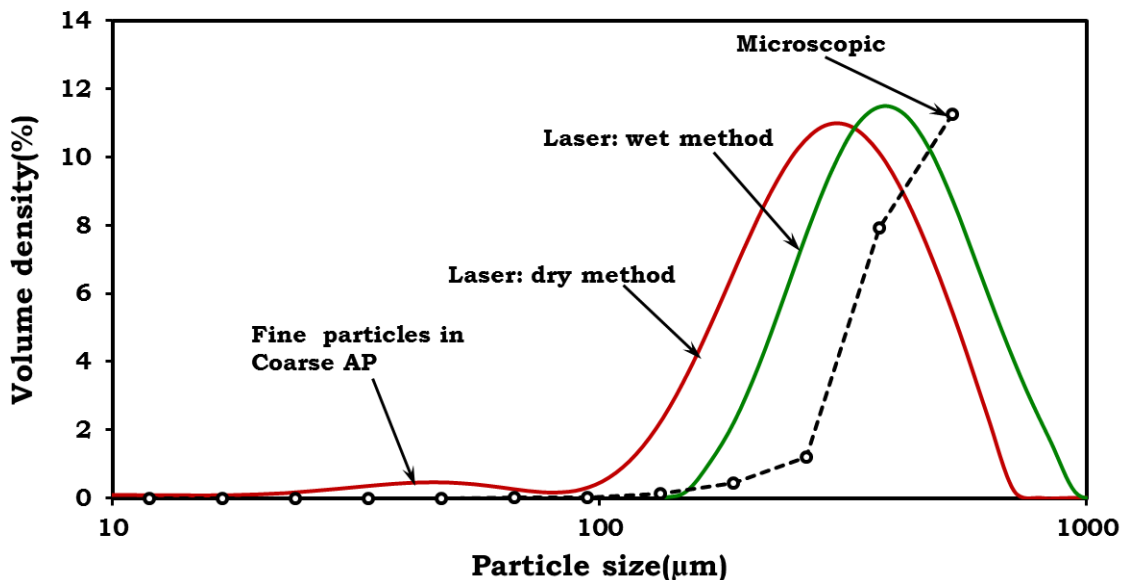


Figure 2.23: Particle size distribution of AP Coarse comparison with image analysis data

It shows that the measured particle size distribution by microscopic analysis is more

biased towards the coarse particles. However, for fine particles (AP fine and ultrafine) Figure 2.8 2.9, such bias is not observed and modes for both classes are close to the mode by laser scatter dry method.

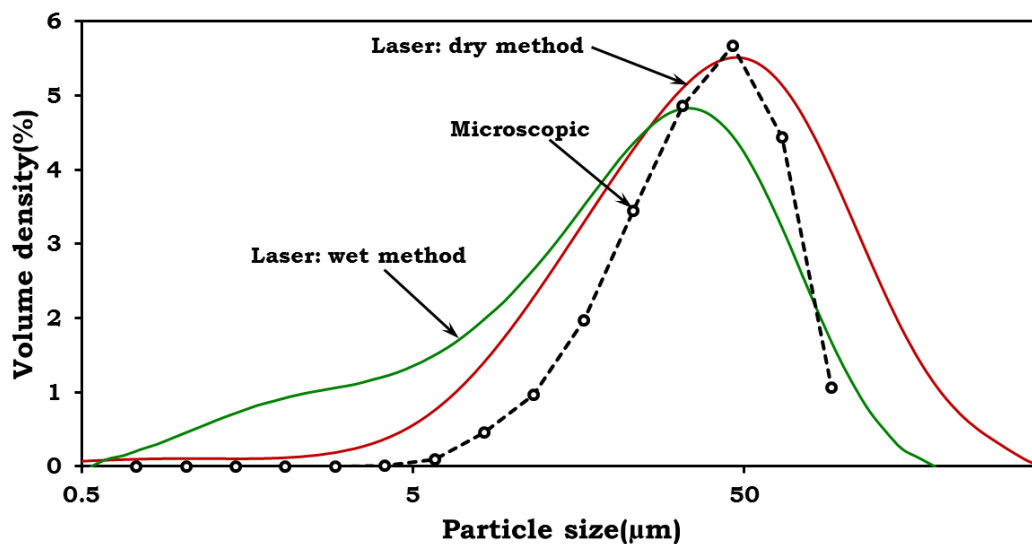


Figure 2.24: Particle size distribution of AP fine comparison with image analysis data

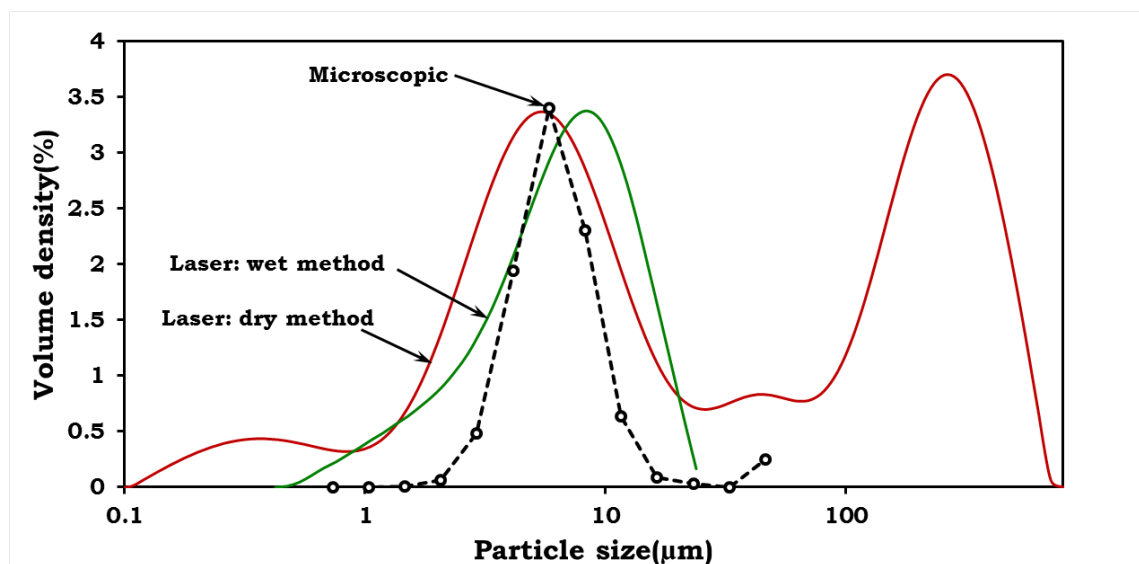


Figure 2.25: Particle size distribution of AP ultra fine comparison with image analysis data

The different methods of particle size distribution measurements can be compared as given in Table 2.5.

Laser Scatter - Dry method	<ol style="list-style-type: none"> <li>1. Easy to carry out test</li> <li>2. Repeatability</li> <li>3. Quick in measurement</li> <li>4. In line with microscopic analysis</li> </ol>
Laser Scatter - wet method	<ol style="list-style-type: none"> <li>1. Better dispersion of particle is possible</li> <li>2. Ultrasound can be applied for breaking cluster</li> <li>3. Elaborate cleaning process is required</li> <li>4. Slow drift in the measurement possibly due to dissolution or grinding during circulation</li> <li>5. Large amount of dispersion liquid is required</li> </ol>
Microscopic analysis	<ol style="list-style-type: none"> <li>1. Direct measurement</li> <li>2. High time consuming</li> <li>3. Low repeatability</li> <li>4. Cumbersome</li> <li>5. gives number distribution</li> </ol>
Sieve analysis	<ol style="list-style-type: none"> <li>1. Well accepted</li> <li>2. Discrete distribution</li> <li>3. Less accurate</li> <li>4. Not effective for fine particle analysis</li> </ol>

Table 2.5: Comparison of different techniques of PSD measurements

## 2.6 Representation of particle size distribution

A typical report of mono modal particle size distribution measured by using laser scatter technique is shown in Figure 2.26. However, this report does not give the standard deviation or dispersion of a particular mean and in such cases the representation of particle size distribution need to be in a better and meaningful way.

There are many ways of representing the particle size distribution data of a particular sample. In the present analysis it is assumed that a particular multi modal distribution of particle is a mixture of several mono modal distributions of particles. A mono modal distribution may follow the log-normal distribution with single mode. Or, mathematically the combination of these mono-modal distribution can be represented by the equation 2.1.

$$[h!]\varphi(x) = \frac{1}{\sqrt{2\pi}} \sum \frac{a_i}{\sigma_i} \exp - \left\{ \frac{x - \mu}{\sqrt{2}\sigma_i} \right\}^2 \quad (2.1)$$

where

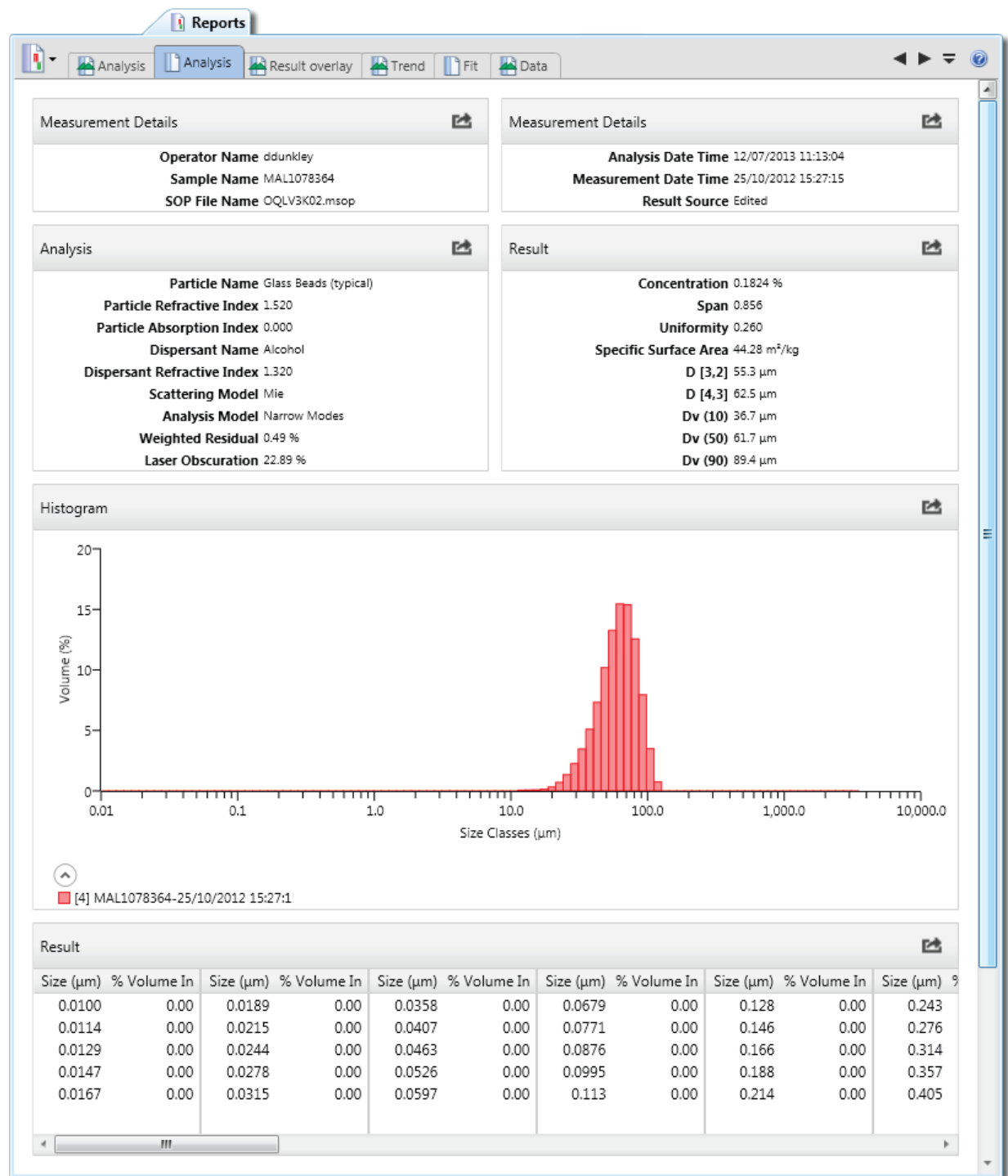


Figure 2.26: A typical report of particle size distribution by Laser scatter

$\varphi$  = Volume density (%)

$\sigma$  = Standard deviation

$\mu$  = Mean

$i$  = Mode representation ( $i^{th}$  modal distribution)

$a$  = volume fraction of particular modal distribution of particles

$x$  = Logarithm of particle size

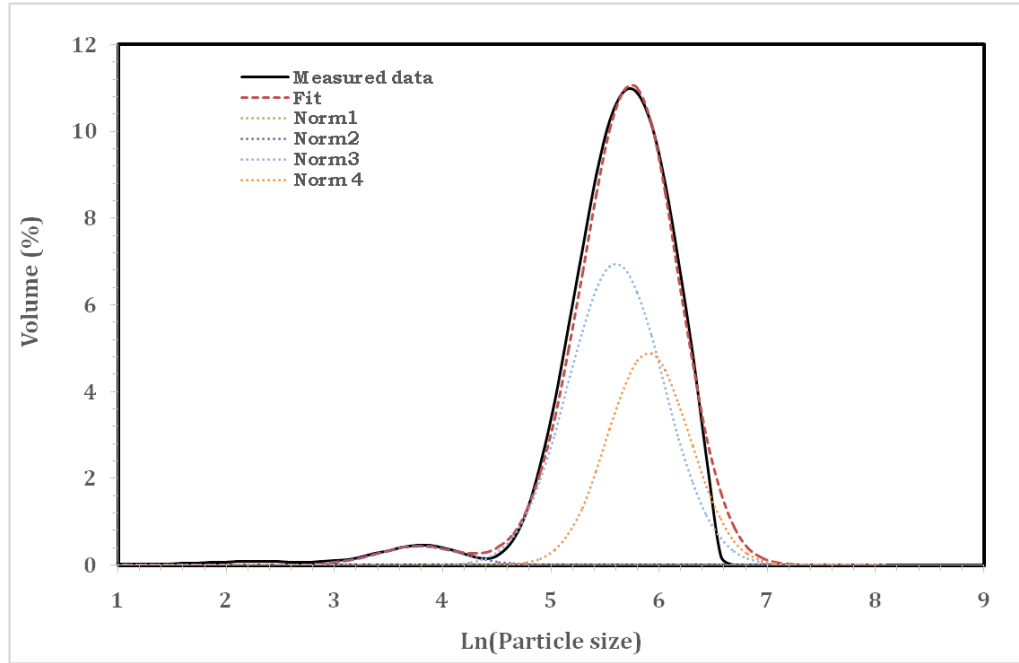


Figure 2.27: Representation of Multi-modal particle size distribution of AP coarse particles

	Mode 1	Mode 2	Mode 3
Mean size ( $\mu\text{m}$ )	43.95	270.43	365.04
Volume (%)	3.5	60	36.5
Standard Deviation	0.4	0.44	0.38

Table 2.6: Parameters of PSD of AP coarse shown in Figure 2.27

It is to be noted that all the three classes of ammonium perchlorate here are multi modal and is not appropriate to represent the distribution with a single volume weighted mean. Hence to make the representation more meaningful, a method of representing the data in terms of volume fraction of particles with a particular mode and standard deviation is proposed. Here the data is fitted to multiple log- normal distribution fits (Gaussian fit) and merging all into one equation. In other words, the results can be read as, the AP coarse particles contain 3.5%, 60% and 36.5% of three

modes of particles with modes 43.94 , 270.43, 365.03  $\mu\text{m}$ . These modes of particle have dispersion with standard deviations of 0.4, 0.44, and 0.38 respectively as shown in Table 2.27.

Similarly, the results for AP Fine and AP Ultrafine are also shown in Figure 2.28 and Figure 2.29 respectively and their corresponding interpretation in tables 2.7 and 2.8

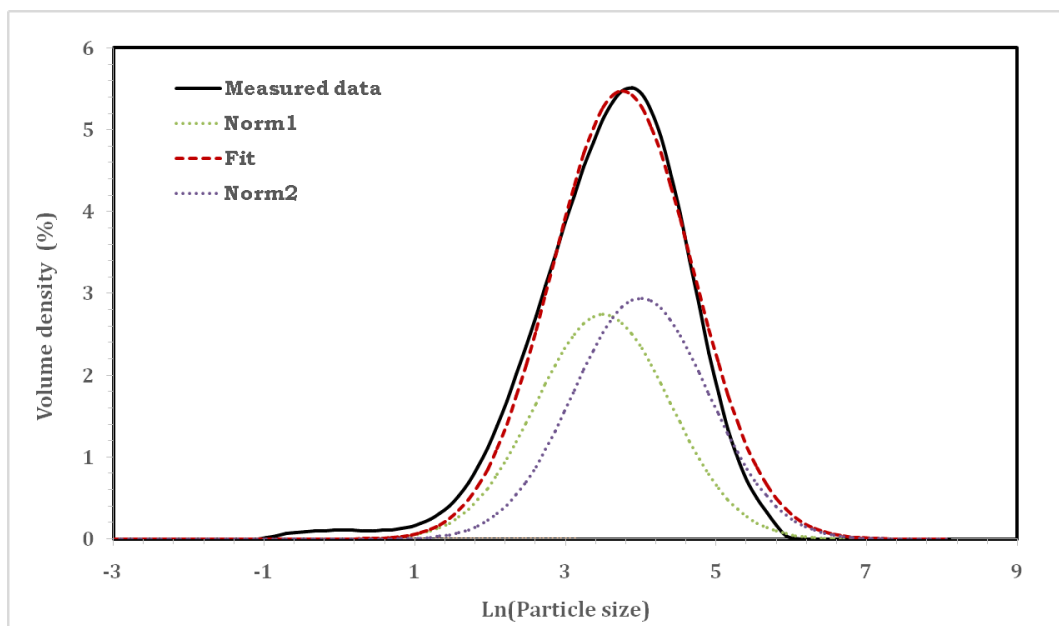


Figure 2.28: Representation of Multi-modal particle size distribution of AP fine particles

	Mode 1	Mode 2
Mean size ( $\mu\text{m}$ )	33.12	54.60
Volume (%)	48	52
Standard Deviation	0.89	0.9

Table 2.7: Parameters of PSD of AP coarse shown in Figure 2.28

	Mode 1	Mode 2	Mode 3	Mode 4	Mode 5
Mean size ( $\mu\text{m}$ )	0.37	5.47	44.70	244.69	164.02
Volume (%)	6	51	8	28	7
Standard Deviation	0.7	0.75	0.42	0.54	0.4

Table 2.8: Parameters of PSD of AP coarse shown in Figure 2.29



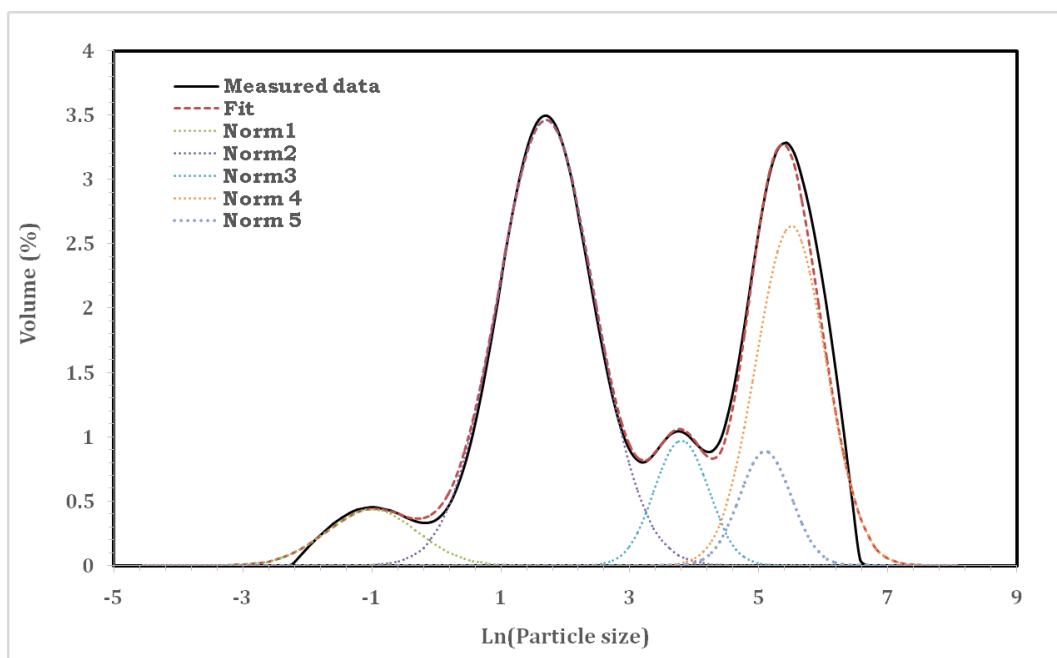


Figure 2.29: Representation of Multi-modal particle size distribution of AP ultra-fine particles

# Chapter 3

## Heterogeneous Quasi One Dimensional (He-Qu-1D) model and Ultrasonic Burning Rate (UBR) technique

### 3.1 Heterogeneous Quasi One dimensional (He-Qu-1D) model

As discussed in the introduction (chapter 1) a valid tool for solid propellant burning rate prediction is an advantage for a designer to develop a new solid propellant composition. The heterogeneous quasi one dimension model (He-Qu-1D) proposed by Varunkumar et.al. [11, 10, 12] where there is no complex computational approach which required huge time and resources, but take into account the diffusion process accurately like [6, 7, 20]. In addition, to the adoption of concepts of Hermance [2] and BDP [3] model, the He-Qu-1D model is also assumed that combustion process is limited between: 1) the premixed flames around coarse AP particles and 2) the premixed flame above very fine AP-binder mix.

This model consists of three parts 1) multi modal propellant geometry 2) 1D deflagration model for pure AP and homogenous propellant, 3) quasi 1D deflagration model for binder matrix coated AP particles.

### 3.1.1 Multi modal AP geometry in propellant

#### Approximating the binder thickness

AP particles in propellant is distributed with different sizes  $d_i$  with corresponding mass fractions  $f_i$ , such that  $\Sigma f_i = \text{SL}$ , where SL is the total AP solid loading in the propellant. Mass fraction of aluminum is  $f_{Al}$  and the mass fraction of binder matrix is termed as  $f_{HTPB} = 1 - \text{SL}$ . From the work of Gross et al. [6] it is understood that as the pressure increases the behaviour of smallest particle size in combustion changes and diffusion effects starts to play a role. Hence a premixed limit diameter  $d_{pm}$  is the diameter below which diffusional effects are neglected and this is a function of pressure as shown in Eq. 3.1. Similarly, the particles undergo local extinction due to fuel rich pockets is also homogenized with binder and its limit is termed as  $d_{ex}$ . All put together this mixture of HTPB, aluminium, critical premixed particles and extinct particles is termed as binder matrix.

$$d_{pm} = 16.7 \exp^{0.02p} \quad (3.1)$$

The thickness  $t_{bm}$  of the binder matrix coated around the AP particles is determined from the Eq. 3.2. LHS of this equation is the total volume of the binder matrix and RHS is the same volume coated uniformly over the rest of the AP particles.

$$\frac{f_{HTPB}}{\rho_{HTPB}} + \frac{f_{pm} + f_{ex}}{\rho_{AP}} + \frac{f_{Al}}{\rho_{Al}} = \sum_{i=1}^n \frac{f_i [(1 + 2t_{bm}/d_i)^3 - 1]}{\rho_{AP}} \quad (3.2)$$

#### Statistical particle path

Consider a random line drawn through a propellant pack. This line will intersect with AP particles of different sizes. The average length fraction ( $l'_i$ ) of this random line that will intersect with AP particles of size  $d_i$  is equal to the corresponding volume fraction ( $V_i$ ), as shown in [22]. Therefore the average number of AP particles of size  $d_i$  along a line will be  $n_i = l_i/d_i = V_i/d_i$ . With each particle coated with binder-matrix of thickness  $t_{bm}$  the diameter of every particle increases by  $2t_{bm}$ ; that is it changes from  $d_i$  to  $d_i + 2t_{bm}$ . Therefore, the length occupied by the particle of size  $d_i$  increases from  $n_i d_i$  to  $n_i (d_i + t_{bm})$ . Since the number of particles are same before

and after binder-matrix coating, the modified length occupied by the particle will be  $V_i(d_i + 2t_{bm}) = d_i$  and the total length of the line will be  $P \sum V_i(d_i + 2t_{bm}) = d_i$ . Using this the line average intersection  $l_i$  for binder-matrix coated AP particle of size  $d_i$  is calculated using Eq.3.3.

$$l_i = \frac{V_i(1 + 2t_{bm}/d_i)}{\sum_{i=1}^n V_i(1 + 2t_{bm}/d_i)} \quad (3.3)$$

Using this  $l_i$  obtained from Eq. 3.3 the propellant burning rate of  $\dot{r}$  can be expressed in Eq.3.4

$$\dot{r} = \left[ \sum_{i=1}^n l_i \dot{r}_i \right] \quad (3.4)$$

### 3.1.2 Pure AP 1D deflagration

The  $\dot{r}_i$  in Eq. 3.4 is to be found to determine the propellant burning rate. Hence the deflagration of pure AP is modelled using heat flux balance as shown in Figure 3.1

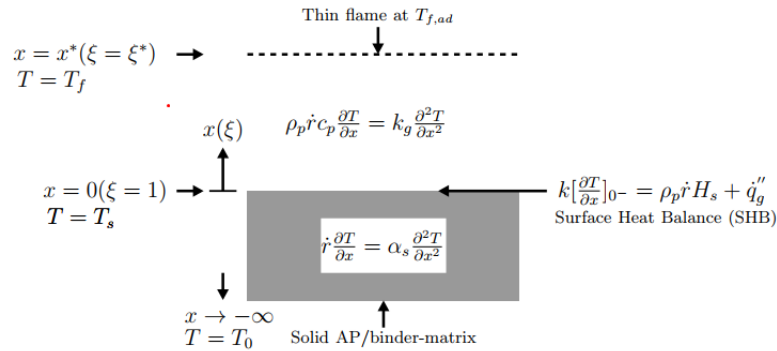


Figure 3.1: Pure AP combustion

The deflagration of AP is considered 1D with a thin premixed flame transferring heat to the surface of condensed phase. AP combustion mechanism consists of two steps 1) exothermic decomposition of AP at propellant surface 2) gas phase reaction between

AP decomposition products. Surface heat balance is represented in Eq.

$$k \left[ \frac{\partial T}{\partial x} \right]_{0^-} = \rho_P \dot{r} H_s + k_g \left[ \frac{\partial T}{\partial x} \right]_{0^+} \quad (3.5)$$

Thus by solving the above equation and Arrhenius type pyrolysis law as given in [12] with boundary conditions, we get a final Eq.3.6 to determine the  $\dot{r}$ .

$$\rho_p \dot{r} = \sqrt{\frac{k_g}{c_p} K_r p^{n_r} \ln \left[ 1 + \frac{T_f - T_s}{T_s - T_0 - \frac{H_s}{c_p}} \right]} \quad (3.6)$$

where

$\rho_p$  = propellant density

$\xi$  = non dimensional number of  $x$

$k_g$  = gas phase thermal conductivity

$c_p$  = condensed phase specific heat at constant pressure

$K_r$  = gas phase reaction rate

$p$  = pressure

$n_r$  = gas phase reaction rate order

$T_f$  = adiabatic flame temperature

$T_s$  = surface temperature

$T_0$  = initial temperature

$H_s$  = net enthalpy change at surface due to phase change

It is assumed that binder matrix thickness of all sized particles is same. This leads to a phenomenon of local extinction because for smaller particles the thickness of binder matrix is large and thus the surface temperature is decreased and below a limit under which the deflagration of the AP cannot exist and are quenched. This limit is termed as low pressure deflagration limit(LPDL) and this phenomenon is termed as local extinction. At some instances the binder being a polymer is decomposed and produce high molecular weight fragments and thus block the heat feedback to the burn surface. This in turn does not allow the binder to vaporise and thus a melting effect is witnessed. This is termed as binder melt. Further the equations and boundary conditions application and other aspects of this model is detailed in [11] and [10].

### 3.1.3 Quasi 1D deflagration of binder matrix coated AP particles

Most practical propellants contain binder-matrix which has solid loading lower than 30%. Binder-matrix with such low loading cannot undergo self-sustained deflagration which implies that the flame above the deflagrating AP particle surface transfers heat only to the central core of the binder-matrix coated AP particle. Therefore, geometric factor,  $g_f$ , which takes care of aforementioned fact, is taken as the area ratio of the mid plane of the AP particle and binder-matrix coated AP particle which can be written mathematically as:

$$g_f = \left( \frac{d_i}{d_i + 2t_{bm}} \right)$$

#### Extent of lateral diffusion and effective flame temperature

The effective temperature of heat transfer to the particle is dependent on the extent of lateral diffusion of AP and binder decomposition products into each other. Hence an lateral diffusional distance is a function of pressure and binder matrix thickness. Finally by replacing the temperatures with effective temperatures and including the geometric factor in Eq. 3.6 we get the final burning rate of the binder matrix coated AP particles.

### 3.1.4 Effect of burning rate modifiers

Burning rate modifiers can be used to either enhance or decrease the burning rate as per the requirement and choice. Iron oxide (IO), Copper Chromite (CC) and activated carbon (ACR) are the most common catalysts. Catalysts enhance the burn rate, predominantly by acting on the gas phase reaction between the decomposition products of HTPB and AP, since they are mixed with the binder during processing. The fact that the pressure index is only marginally affected by addition of catalyst is indicative of the predominant gas phase effect. This can be accounted for in the current framework by suitably modifying the activation energy of the gas phase reaction. The extent to which the activation energy must be decreased, which will be a function of the catalyst concentration, can be estimated from the measured burn rate enhancement of fine AP/HTPB premixed propellant with increasing fraction of

catalyst. Information on the saturation limit of catalysis can also be obtained from the same data.

**Note:** The detailed explanation with equations and figures of the He-Qu-1D model is given in [11, 10, 12]

## 3.2 Ultrasonic burn rate (UBR) technique

A new technique of measuring the burning rate of solid propellant developed by Jeenu et. al. [23] in VSSC and is being used for the characterization of all the solid propellants of ISRO. This is based on the pulse echo ultrasonic technique. The specimen quantity required is as small as 60 grams as shown in Figure 3.2

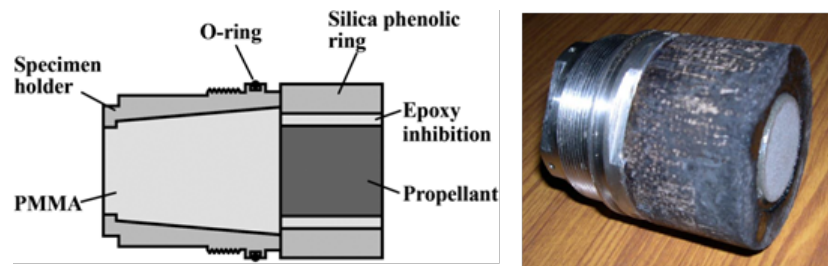


Figure 3.2: Propellant specimen of UBR bonded in specimen holder.

The test set up used for the measurement of all the propellant formulations to be discussed later in this thesis is shown below in Figure 3.3. Further the technique of testing and procedure is clearly elaborated in [23].



Figure 3.3: Ultrasonic burning rate test set up



# Chapter 4

## Model predictions and experimental data of composite solid propellant compositions

The attempt was to validate the He-Qu-1D model for the ISRO solid propellant formulations and thus make this as a predictive tool so that it would be useful tool for future new formulations which would emerge out with minimum tests required for qualification. The model equations presented in [12] and [10] are implemented in MATLAB. In the present study, 6 compositions were taken into consideration for validation of the model as shown in the Table 4.1. Using the model (updated MATLAB code) the burning rates of different propellant compositions were predicted and compared with experimental results of UBR. Particle size distribution of ammonium perchlorate measured using laser diffraction technique in Malvern Mastersizer 3000 located in Rocket Propellant Plant (RPP) / VSSC were used for the model prediction. All the experimental results are measured by ultrasonic burning rate facility in Propellant Engineering Division (PED) / VSSC

### 4.1 Results and Discussion

Out of these six compositions, two compositions (type 1 and type 2) were taken without catalyst and remaining all are of catalysed formulations for the present study. However, all the compositions taken into consideration consists of aluminium at different concentrations. The following are the predictions and its experimental results plotted.

Composition	Burning rate class	Approx. Burning rate @ 40 kgf/cm <sup>2</sup>	Catalyst	AP distribution (C:F:UF)	Pressure index (n)
Type 1	Slow	5.6 mm/s	None (0%)	4:1:0	0.37
Type 2	Slow	5.8 mm/s	None (0%)	3:1:0	0.36
Type 3	Medium	8.3 mm/s	CC (0.25%)	2:1:0	0.43
Type 4	High	13.0 mm/s	CC (1%), IO (1%)	0:1:0	0.43
Type 5	High	16.3 mm/s	CC (1%), Fe <sub>2</sub> O <sub>3</sub> (1%)	2:3:1	0.437
Type 6	High	11.0 mm/s	CC (1%)	1:1.2:0	0.385

Table 4.1: Different compositions taken for the prediction

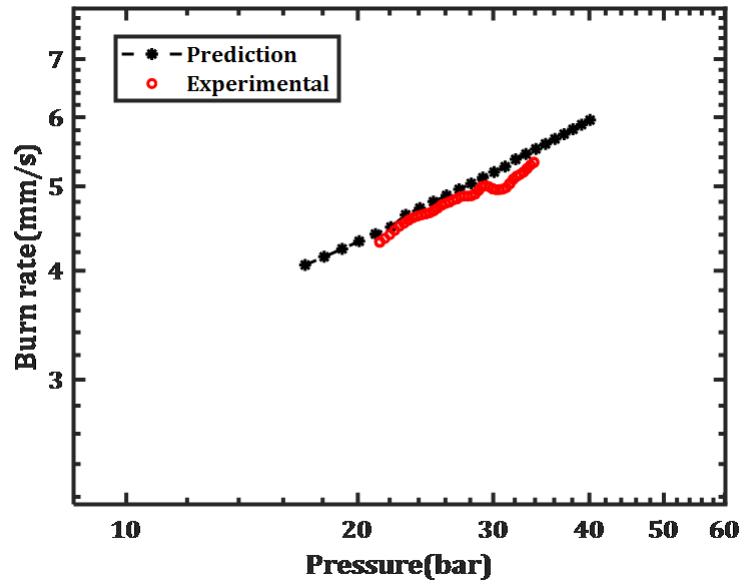


Figure 4.1: Prediction and Experimental data of Type 1 propellant composition

Predictions of all these formulations as shown in Figures 4.1 to 4.6 are found to be in good agreement with the experimental results. However, it is to be noted that the activation energy has been taken as a linear fit between the two limiting conditions of 1) composition of without any catalyst and 2) composition with catalyst concentration added up to the saturation limit, beyond which catalyst cannot influence the burn rate.

In order to study the effect of catalyst in the propellant composition and to validate the same with predictions, propellant type 3 in Table 4.1 has been chosen and new mix

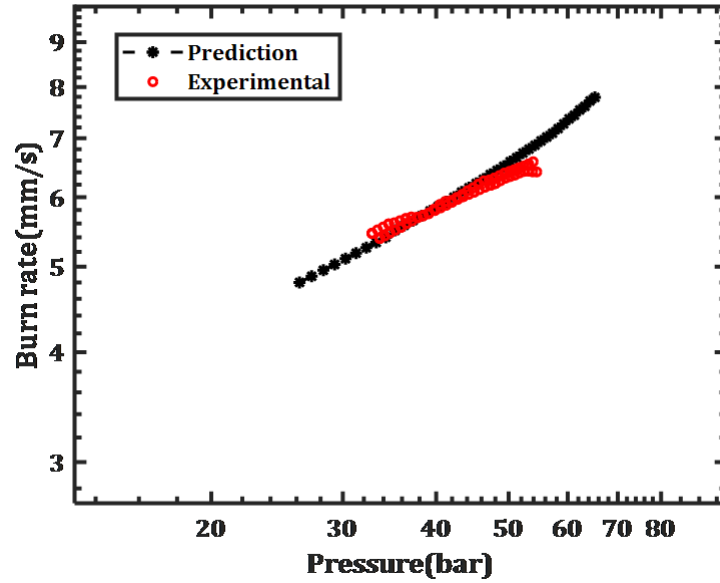


Figure 4.2: Prediction and Experimental data of Type 2 propellant composition

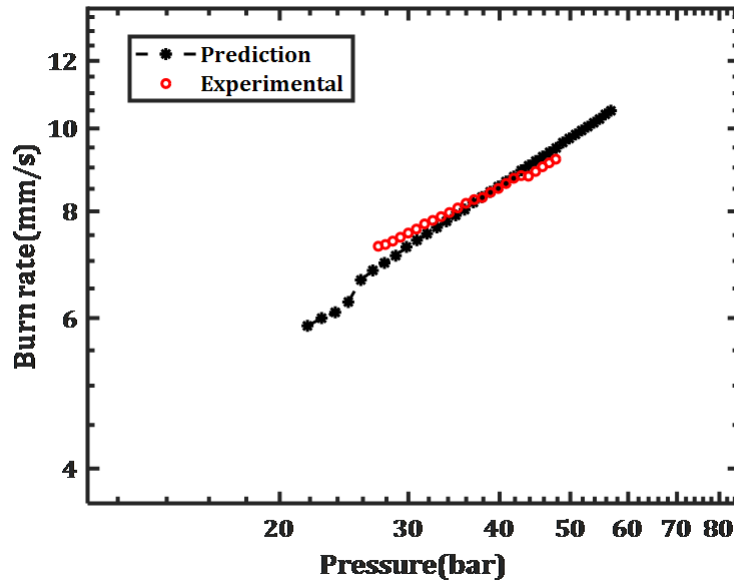


Figure 4.3: Prediction and Experimental data of Type 3 propellant composition

was processed by removing the catalyst and compensating the catalyst concentration (0.25%) with equal amounts of AP coarse and AP fine in the same proportions. The experimental and predictions are shown in Figure 4.7

From the Figure 4.7 it is observed that the catalyst effect has been clearly captured by the model. However, there is a little difference between the experimental and prediction results, but marginal.

Type 5 propellant consists of 20 % ultrafine AP in addition to 30% and 20% fine

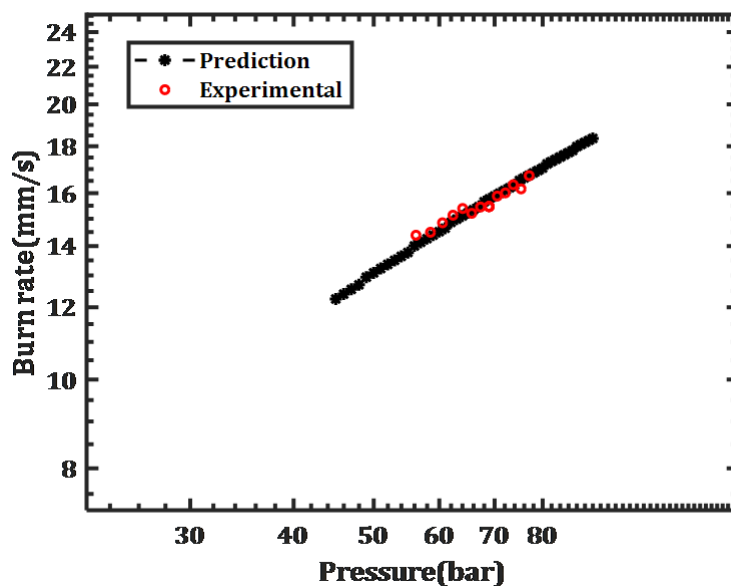


Figure 4.4: Prediction and Experimental data of Type 4 propellant composition

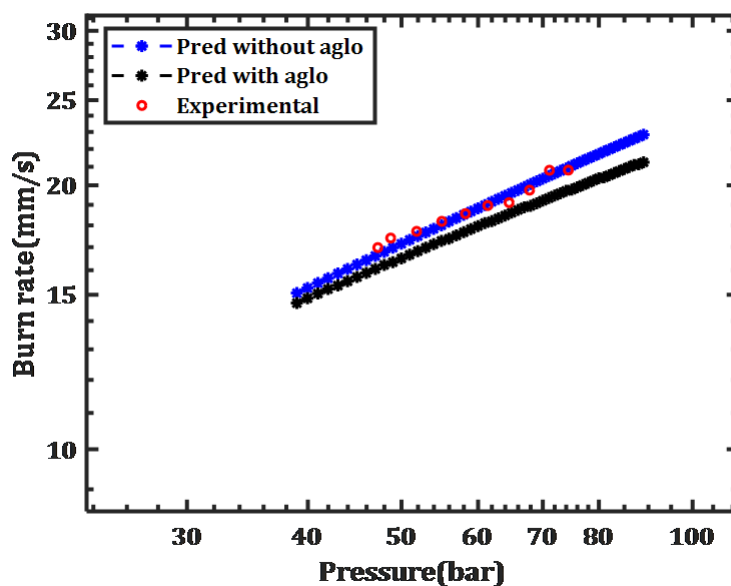


Figure 4.5: Prediction and Experimental data of Type 5 propellant composition

and coarse AP respectively. Measurement of PSD of these ultrafine particles using dry method gives a bi modal distribution in which the coarser mode of the distribution corresponds to agglomeration of the ultrafine particles. In view of this, predictions were generated with and without the agglomeration data as shown in Figure 4.5. These two predictions are marginally different and lie in the dispersion range of the propellant burn rate. For type 6 propellant we observe that there is a change in slope in the prediction data with respect to experimental. There was limited data

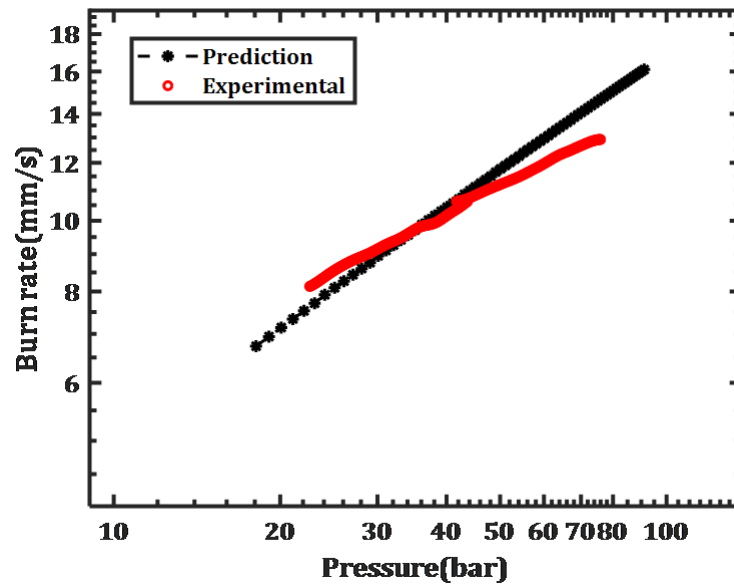


Figure 4.6: Prediction and Experimental data of Type 6 propellant composition

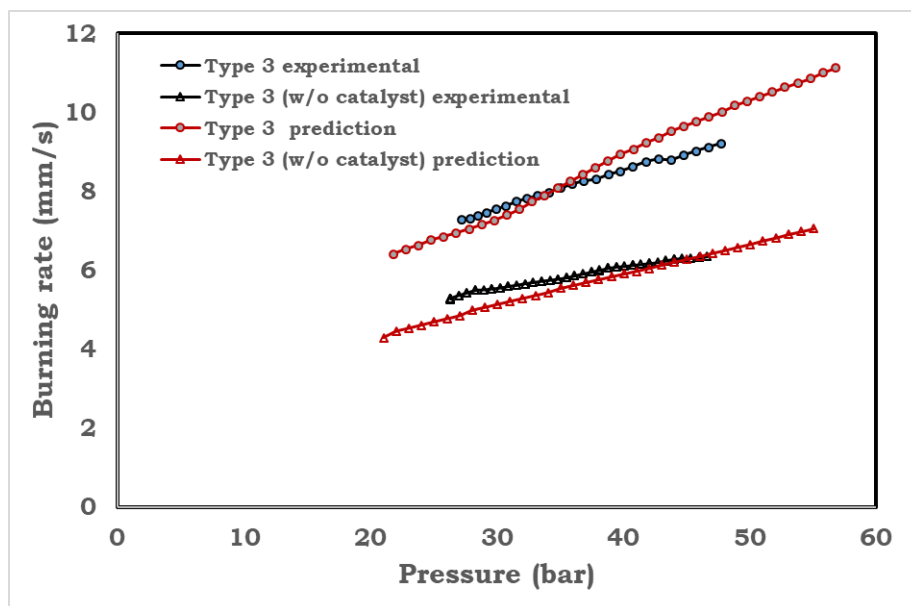


Figure 4.7: Predictions and experimental results of Type 3 propellant with and without catalyst.

available on this composition and hence it has to be studied in details with more data generation.

## 4.2 Comparison of predictions with PSDs from wet and dry method of laser scatter

From the analysis of particle size distribution in the chapter 2, it was concluded that dry method of laser scatter technique is more easy and accurate method of measurement. However to account the effect of the variation of PSD by both wet and dry method, predictions were generated using both and is compared with experimental results for Type 1, Type 2, Type 4 and Type 5 as shown in Figures 4.8,4.9, 4.10 and 4.11 respectively.

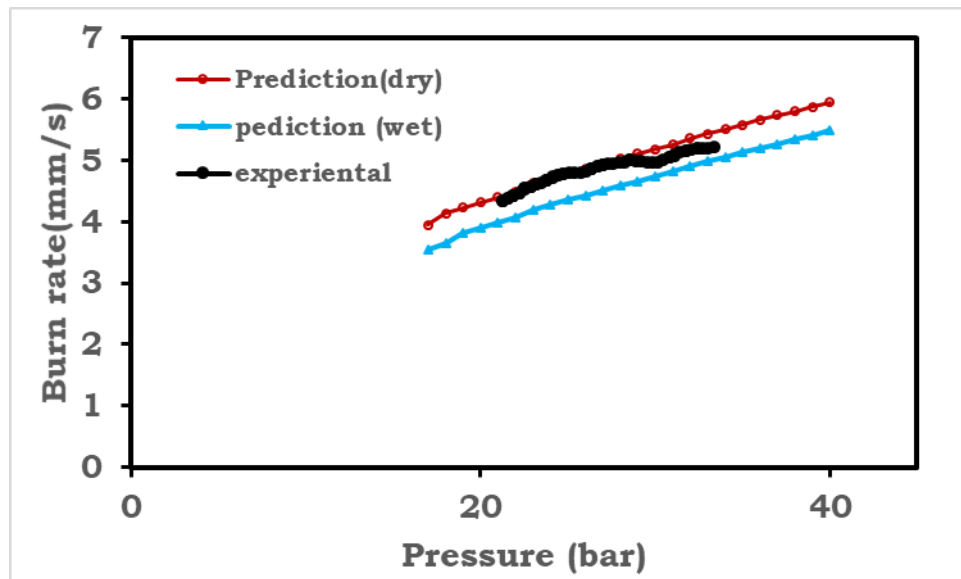


Figure 4.8: Comparison of prediction with PSDs measured by laser scatter wet method and dry method and experimental results of Type 1 propellant

From these results it is quite evident that laser scatter dry method is truly representing the particle size distribution of AP in the propellant mix as far as this model is concerned. The PSD of both the methods are plotted in Figure 4.12 and the Figure 4.13 shows the difference of the PSDs of both the dispersion techniques when all the classes of AP is considered. The master curves shown in Figure 4.13 shows that fine fraction of AP is higher when the same material is analysed by Laser scatter wet method as compared to dry method.

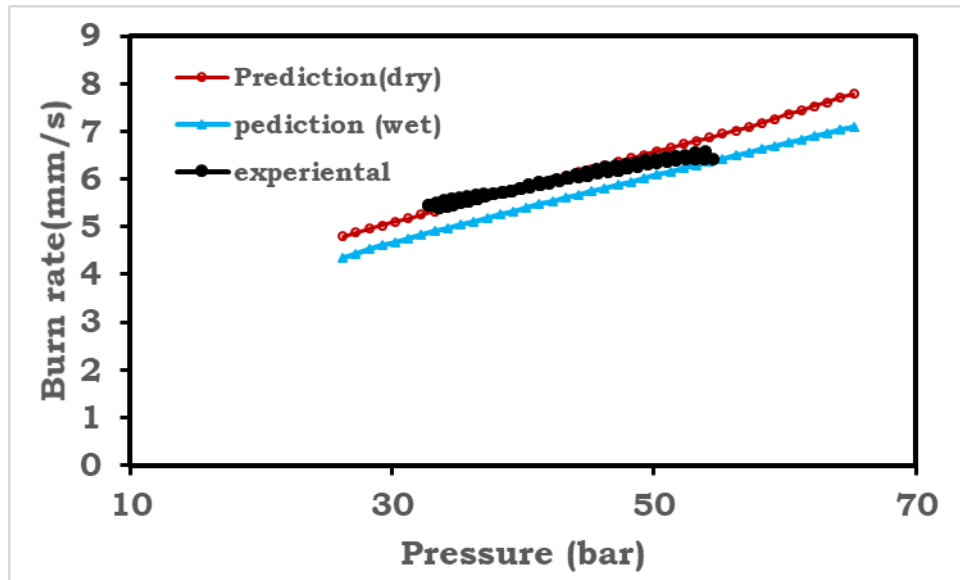


Figure 4.9: Comparison of prediction with PSDs measured by laser scatter wet method and dry method and experimental results of Type 2 propellant

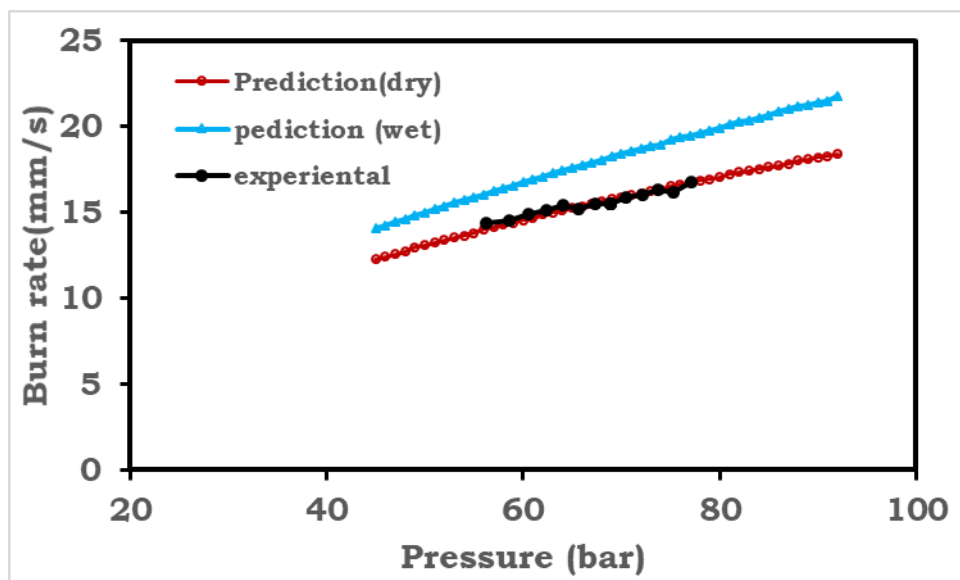


Figure 4.10: Comparison of prediction with PSDs measured by laser scatter wet method and dry method and experimental results of Type 4 propellant

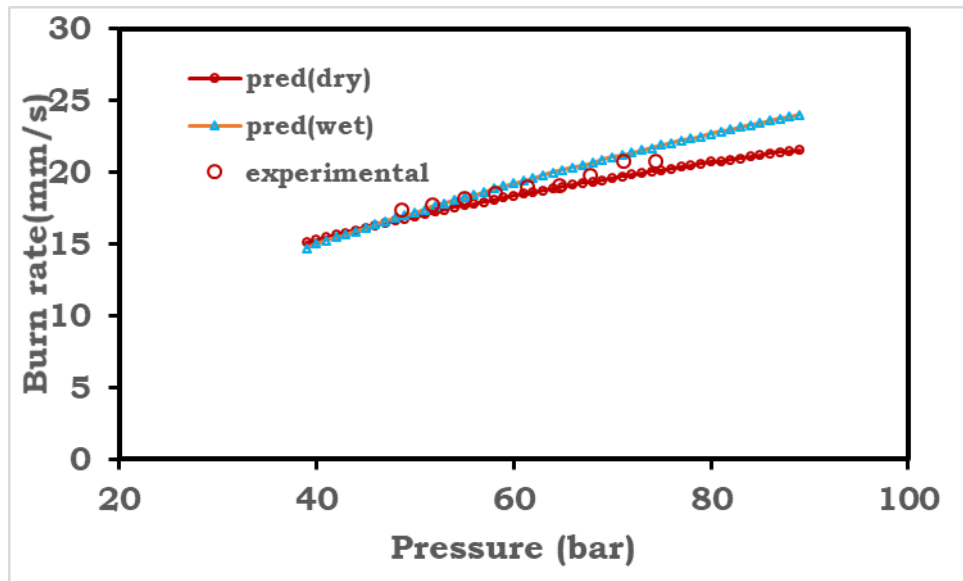


Figure 4.11: Comparison of prediction with PSDs measured by laser scatter wet method and dry method and experimental results of Type 5 propellant

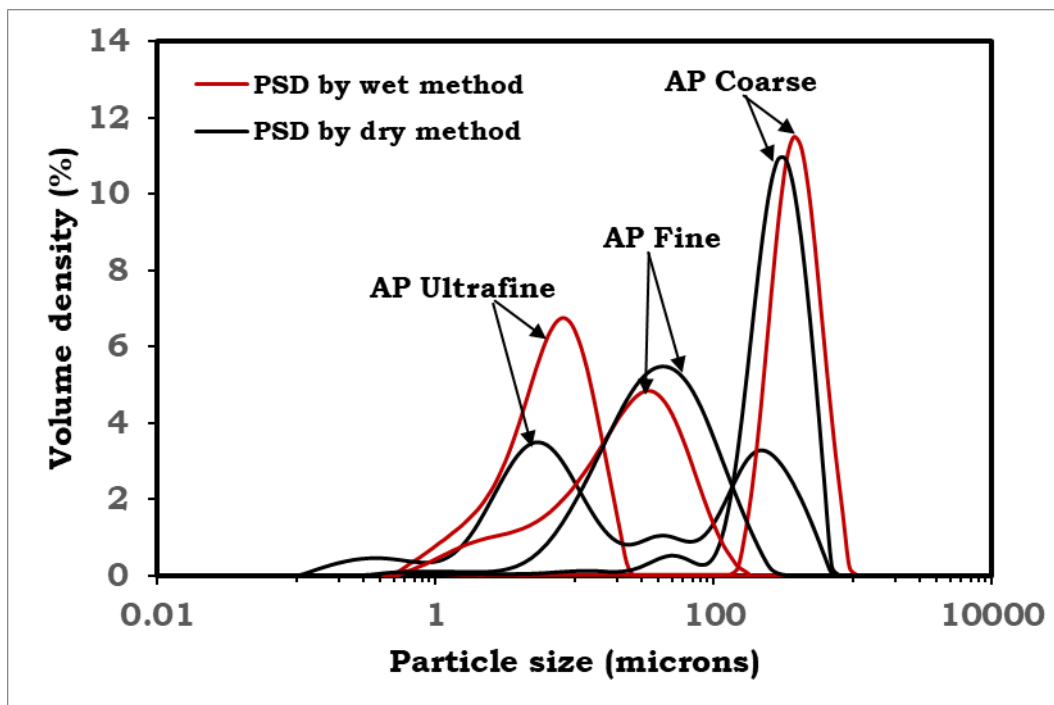


Figure 4.12: Comparison of PSD of all classes of AP measured by both Laser scatter wet and dry methods



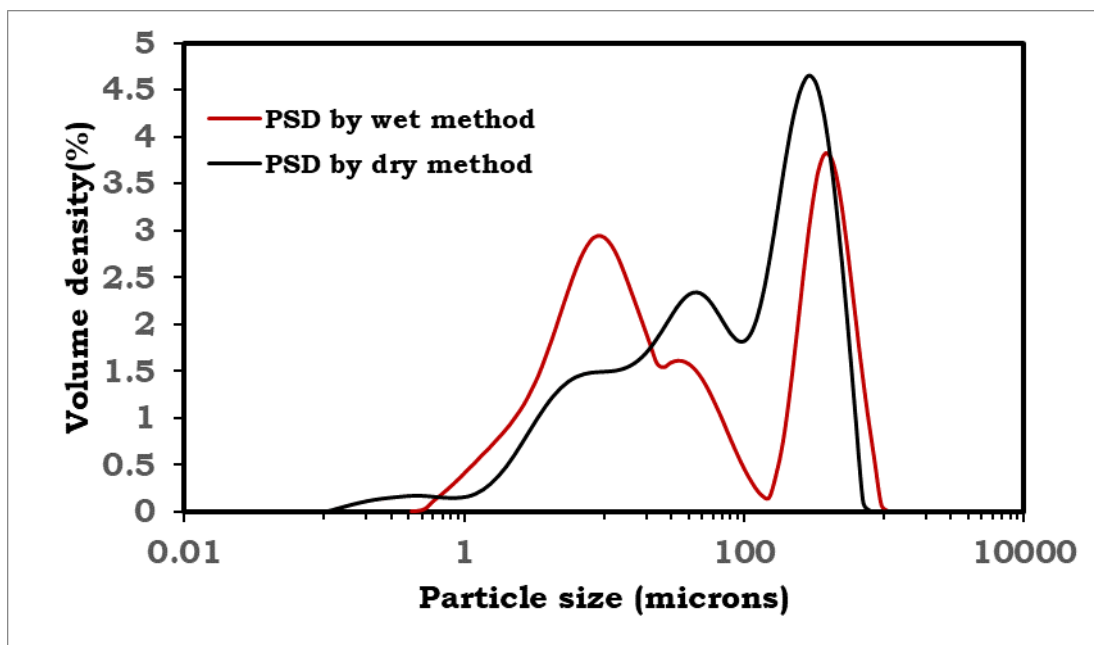


Figure 4.13: Comparison of master PSD curve of AP by integrating all the classes.

# Chapter 5

## Conclusion and future work

From all the above analysis covering different types of measurement techniques of particles size distribution in particular of ammonium perchlorate the following conclusions can be made.

- The whole exercise or study carried out was to evolve a definite and accurate methodology for the measurement of PSD of AP all classes repeatedly.
- AP needs to be considered special case of material being moisture sensitive and fragile in nature.
- Dry method of laser scatter is found to be more reliable, repeatable and faster method to analyze particle size distribution.
- Comparison with sieve and microscopic analysis with laser scatter-dry method showed good agreement.
- Aspect of clustering of the particles also has to be considered especially in the case of AP ultrafine. The information of the extent of clustering in ultrafine AP particles is available in the dry analysis.

The heterogeneous quasi one dimensional burn rate prediction model is used to compare with the experimental results of about six compositions and had shown comparable predictions compared to the experimental results for all the formulations considered. However, few aspects are to be still fine-tuned and incorporated in the model to make it still stronger and universal so as to be used as a predictive tool by the designer of the solid propellant. In this context the following studies are being proposed for future.

1. Prediction and its experimental results of a standard solid propellant composition of 86% AP 14% HTPB without any aluminium or catalyst to evaluate catalyst effects. The following are the recommended compositions
2. With the standard formulation said above it is proposed to add catalyst at different concentration and use this data in the model.
3. Taking into account the binder melt in compositions in particular where the concentrations of fine AP powders are dominating. This may further fine tune and enhance the predictive capability of this model.

# References

- [1] C. E. Hermance. A Model of Composite Propellant Combustion Including Surface Heterogeneity and Heat Generation. *AIAA Journal* 4, (1966) 1629–1637.
- [2] C. Hermance. A detailed model of the combustion of composite solid propellants.
- [3] M. Beckstead, R. Derr, and C. Price. The combustion of solid monopropellants and composite propellants. In Symposium (International) on Combustion, volume 13. Elsevier, 1971 1047–1056.
- [4] N. S. Cohen and D. A. Flanigan. Mechanisms and models of solid-propellant burn rate temperature sensitivity-A review. *AIAA journal* 23, (1985) 1538–1547.
- [5] N. S. Cohen. Review of composite propellant burn rate modeling. *AIAA Journal* 18, (1980) 277–293.
- [6] M. Gross. Towards a predictive propellant burning rate model based on high-fidelity numerical calculations. In 46th AIAA/ASME/SAE/ASEE Joint Propulsion Conference & Exhibit. 2010 6914.
- [7] M. L. Gross and M. W. Beckstead. Diffusion flame calculations for composite propellants predicting particle-size effects. *Combustion and Flame* 157, (2010) 864–873.
- [8] R. Miller. Effects of particle size on reduced smoke propellant ballistics.
- [9] C. V. Kumar Nagendra and P. Ramakrishna. Three-dimensional heterogeneous propellant combustion. *Proceedings of the Combustion Institute* 37, (2018) 3151–3158.
- [10] S. Varunkumar and H. Mukunda. Aluminized composite propellant combustion modeling with Heterogeneous Quasi-One dimensional (HeQu1-D) approach. *Combustion and Flame* 192, (2018) 59–70.

- 
- [11] S. Varunkumar, M. Zaved, and H. Mukunda. A novel approach to composite propellant combustion modeling with a new Heterogeneous Quasi One-dimensional (HeQu1-D) framework. *Combustion and Flame* 173, (2016) 411–424.
- [12] M. Z. Siddiqui. Heterogeneous quasi one dimensional model for steady state combustion of AP/HTPB based composite propellants .
- [13] M. Beckstead. A model for solid propellant combustion. In Symposium (International) on Combustion, volume 18. Elsevier, 1981 175–185.
- [14] R. Kelly and F. Etzler. What is wrong with laser diffraction. *A critical review of current laser diffraction methods for particle size analysis. Donner Technologies*, [http://www.donner-tech.com/whats\\_wrong\\_with\\_ld.pdf](http://www.donner-tech.com/whats_wrong_with_ld.pdf) .
- [15] M. Li, D. Wilkinson, and K. Patchigolla. Comparison of particle size distributions measured using different techniques. *Particulate Science and Technology* 23, (2005) 265–284.
- [16] T. J. Davies. particle size measurement and interpretation. Technical report of queensland alumina limited.
- [17] S. Jain, D. Mehilal, S. Nandagopal, P. Singh, K. Radhakrishnan, and B. Bhattacharya. Size and Shape of Ammonium Perchlorate and their Influence on Properties of Composite Propellant. *Defence Science Journal* 59, (2009) 294–299.
- [18] G. Eshel, G. Levy, U. Mingelgrin, and M. Singer. Critical evaluation of the use of laser diffraction for particle-size distribution analysis. *Soil Science Society of America Journal* 68, (2004) 736–743.
- [19] R. Jeenu, K. Pinumalla, and D. Deepak. Size distribution of particles in combustion products of aluminized composite propellant. *Journal of Propulsion and Power* 26, (2010) 715–723.
- [20] M. L. Gross, T. D. Hedman, S. F. Son, T. L. Jackson, and M. W. Beckstead. Coupling micro and meso-scale combustion models of AP/HTPB propellants. *Combustion and Flame* 160, (2013) 982–992.

- 
- [21] M. L. Gross and M. W. Beckstead. Steady-state combustion mechanisms of ammonium perchlorate composite propellants. *Journal of Propulsion and Power* 27, (2011) 1064–1078.
- [22] A. Iyer, N. Balamurali, and S. Varunkumar. Random packing of multi-modal spheres in a cubic box a model for understanding AP/HTPB based composite solid propellants. In International Autumn Seminar on Propellants, Explosives and Pyrotechics, Qingdao, 2015. 2015 .
- [23] R. Jeenu, K. Pinumalla, and D. Deepak. Industrial adaptation of ultrasonic technique of propellant burning rate measurement using specimens. *Journal of Propulsion and Power* 29, (2012) 216–226.